CHALMERS
UNIVERSITY OF TECHNOLOGY

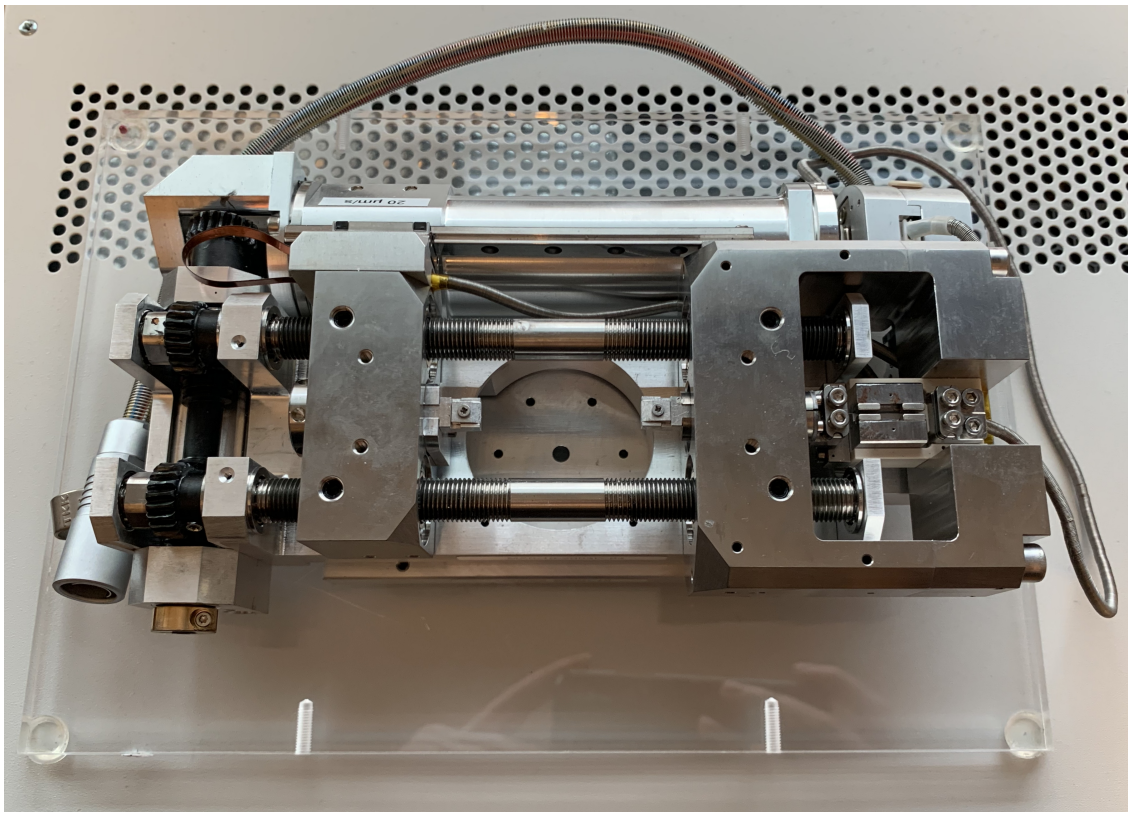

Development of a micromechanical testing method for single wood fibres

Towards a better understanding of the effect of humidity level on the mechanical properties of the fibres

Master's thesis at Master Program Materials Engineering

EMELIE SEIGNÉR

DEPARTMENT OF INDUSTRIAL AND MATERIALS SCIENCE
CHALMERS UNIVERSITY OF TECHNOLOGY
Gothenburg, Sweden 2022
www.chalmers.se

Master's thesis 2022

Development of a micromechanical testing method for single wood fibres

Towards a better understanding of the effect of humidity level on the mechanical properties of the fibres

EMELIE SEIGNÉR

CHALMERS
UNIVERSITY OF TECHNOLOGY

Department of Industrial and Materials Science
Division of Engineering materials
Chalmers University of Technology
Gothenburg, Sweden 2022

Development of a micromechanical testing method for single wood fibres
Towards a better understanding of the effect of humidity level on the mechanical properties of the fibres
EMELIE SEIGNÉR

Supervisor: Fang Liu, Department of Industrial and Materials Science
Examiner: Fang Liu, Department of Industrial and Materials Science

Master's Thesis 2022
Department of Industrial and materials science
Division of Engineering materials
Chalmers University of Technology
SE-412 96 Gothenburg
Telephone +46 31 772 1000

Cover: The tensile machine used in this thesis.

Typeset in LaTeX
Printed by Chalmers Reproservice
Gothenburg, Sweden 2022

Development of a micromechanical testing method for single wood fibres
Towards a better understanding of the effect of humidity level on the mechanical properties of the fibres
EMELIE SEIGNÉR
Department of Industrial and materials science
Chalmers University of Technology

Abstract

Natural fibre-based materials are widely used in everyday life in the form of paper, paperboard, films, textiles and biocomposites. Environmental awareness and the growing concern regarding the large energy consumption coupled to the production of traditional synthetic fibres have prompted several industries to search for sustainable materials to replace the traditional fibres. The usage of natural fibres in high-performance composites necessitates a thorough understanding of their mechanical properties. In this thesis, a robust and high throughput method was developed to conduct tensile tests on individual single wood fibres. Using this method, wood fibres of industrial origin were investigated, in particular, the effect of the humidity level on the tensile properties of these fibres was studied. Weibull statistics were used to understand the strength and possible defects in microstructure of the fibres. The key conclusion drawn from this study is that with decreased relative humidity level, the strength of the wood fibres increases. Also, fibres exposed to low levels of relative humidity has less defects on the microstructure level than fibres exposed to higher levels of humidity.

Keywords: Single fibre, Wood fibre, Micromechanical testing, Tensile testing, Relative humidity, Weibull statistics, Mechanical properties

Acknowledgements

It has been an educational and interesting Master´s thesis project that has given me a broader understanding of how single fibres behave when exposed to various humidities and it has also been a good deepening in my education. The practical work has given me new experiences and an understanding of how these tests according to standards are done and link it to all the theory I read.

I would like to thank the University and all staff who have made this project possible. A warm special thanks to my supervisor Fang Liu who has been very helpful and supporting throughout the work and given me the opportunity to do a fun and educational job. A big tanks to my opponent Anton for the help with this thesis. Finally I extend a thanks to my family for all the support during this time.

Emelie Seignér, Gothenburg, June 2022

List of Acronyms

Below is the list of acronyms that have been used throughout this thesis listed in alphabetical order:

AFM	Atomic Force Microscopy
ASTM	American Society For Testing And Materials
CSA	Cross-Sectional Area
DIC	Digital Image Correlation
FIB	Focused Ion Beam
IFSS	Interfacial Shear Strength
MFA	Microfibril Angle
NRMSD	Normalization Root-mean-square Deviation
RH	Relative humidity
RMSD	Root-mean-square Deviation
SEM	Scanning Electron Microscope
UTS	Ultimate Tensile Strength
WAXD	Wide-Angle X-ray diffraction

List of Figures

List of Tables

Contents

1
Introduction

Natural fibre-based materials are widely used in everyday life in the form of paper, paperboard, films, textiles and biocomposites. Environmental awareness and the growing concern regarding the large energy consumption coupled to the production of traditional synthetic fibres have prompted several industries to search for sustainable materials to replace the traditional fibres. Wood fibres, a form of cellulose-based fibre, provide excellent prospects for future sustainable reinforcement in polymer composites. Wood fibers are very hydrophilic, meaning they are sensitive to moisture. This is a significant challenge when it comes to wood fibres since it implies poor compatibility with most hydrophobic polymers. To deal with this issue, wood fibers are frequently modified in a variety of ways, including chemical and mechanical. These alterations can change the properties of the fibers, the interface between the fibre and the polymer, and how they interact with one other at different humidity levels. When studying composites, macroscopic testing is the dominant technique when it comes to current research and development of wood fibre reinforced composites today.

Today, a lot of composites are made of carbon fibres or glass fibres. One goal of this project is to help in the development of fast screening of fibres and understand the effect of chemical treatment on the mechanical properties, and provide reliable input on modelling of sustainable wood fibre composites.

1.1 Purpose

The aim of this thesis is to develop a robust and high throughput method to conduct tensile tests on individual single wood fibres. Then, by using this method, wood fibres of industrial origin were investigated, in particular, the effect of moisture exposure on the mechanical properties of these fibres were studied.

1.2 Thesis outline

This thesis begins with a theoretical framework chapter, chapter 2, a detailed description of the methodology behind the results is presented in chapter 3. The obtained results are provided in chapter 4, to be discussed in chapter 5. Finally, conclusions that may be drawn from this thesis and its result are presented in chapter 6. In addition, data from the results is presented the Appendix A.

2
Theoretical framework

This chapter is dedicated to explain the fundamental theory behind the experiments performed in this thesis. In section 2.1, a short introduction to plant fibres and wood materials is presented followed by a short description regarding the different microscopes used in this project in section 2.2. Information regarding Young´s modulus is provided in subsection 2.3 and Weibull statistics is introduced and described in section 2.4.

2.1 Plant fibres and wood fibre materials

This section starts with describing the hierarchical structure of wood in subsection 2.1.1, followed by the effect of moisture absorption on properties of wood fibers in subsection 2.1.2. Mechanical and physical properties of wood fibres is described in subsection 2.1.3, after that, environmental impact and recycled paper is introduced in subsection 2.1.4. And last, in subsection 2.1.5, the standard used in this thesis is described.

2.1.1 Hierarchical structure of wood

The primary chemical components of wood fibres are cellulose, hemicellulose, and lignin at the molecular level and cellulose is the most abundant component in wood fibres. Wood fibres have a significant impact on the ultimate performance of wood at the nanoscopic level. Based on lignin–carbohydrate complex through covalent bonding, wood fibres are made up of cellulose microfibrils (10–25 nm), hemicelluloses, and lignins [1]. Figure 2.1, shows a three-dimensional illustration of wood cell walls and the ether linkage between lignin and carbohydrate [2]. The majority of microfibrils are not parallel to the cell axis and form a certain angle called the microfibril angle (MFA). MFA is a key component in establishing the physical, for example shrinkage, and mechanical, for example, stiffness and tensile strength, qualities of wood fibres [1].

Wood fibres have a hierarchical structure that offers them outstanding performance properties, such as a high strength-to-weight ratio [1]. Figure 2.2 illustrates the hierarchical structure of a wood fibre [3]. The wood fibres are made up of four layers at the ultrastructural level, usually 1–25 μm. There is the primary wall (P), middle lamella (M), secondary wall (S) and the Warty layer (W). There are three layers in the secondary wall S, (S_1), the outside layer of the secondary wall, (S_2), the

middle layer of the secondary wall and (S_3), the inner layer of the secondary wall. The cells are separated by the central lamella and this layer contains a lot of lignin. Around 70%-80% of lignin is in this layer which is roughly twice as much as in the secondary wall. Although the high concentration of lignin can effectively glue the cells together, separation of the remaining lignin on the fibre surface after processing can result in a reduction in inter-fibre bonding. The properties of the primary wall layer vary from those of the secondary wall layer due to the presence of pectin and protein. Significant interactions exist in this layer between the lignin, protein, and pectin, and between the cellulose and hemicellulose. This evident characteristic has a significant impact on fiber separation. The secondary cell wall has a significantly higher number of organized microfibrils than the primary cell wall. The Warty layer (W) has similar in thickness as the primary wall and is made up of four to six lamellae spiralling in opposing directions around the tracheid's longitudinal axis. The outer secondary cell wall S_1 contains closed fibrillar structure and has a significant MFA of around 50°–70°. This is thought to have a major role in defining the transverse mechanical properties and surface characteristics of fibres. The main part of the secondary wall is located in the middle secondary cell wall. This layer's microfibrils spiral sharply around the axial direction with an angle of 5-30° and have a significant impact on fibre characteristics. The thickest cell wall layer, the S_2, regulates the strength of the whole fibre. At the lumen border, the inner secondary wall (S_3, 0.1 μm), also known as the tertiary wall, provides a barrier between the lumen and the remainder of the cell wall. The S_3 layer has the largest concentration of lignin, around 53%. The S_3 layers microfibrils are practically perpendicular to the S_2 layers microfibrils and has a MFA around 50°-90°. The Warty layer, which is made up of protoplasmic waste, covers the deepest region of the cell wall [1].

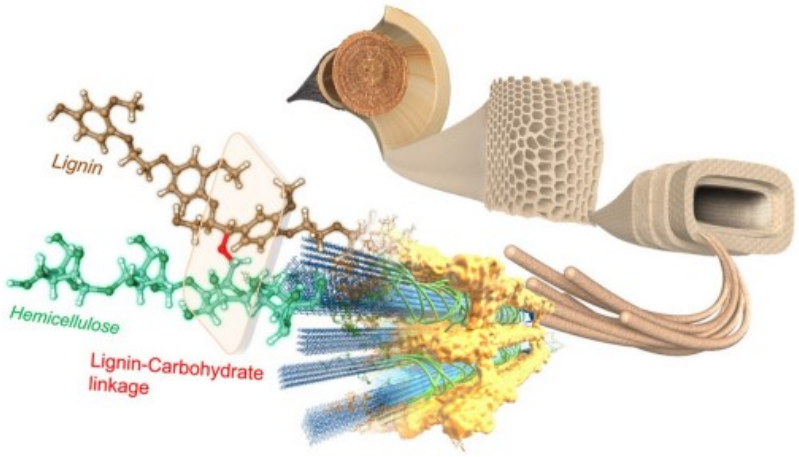

Figure 2.1: A three-dimensional illustration of wood cell walls and the ether linkage between lignin and carbohydrate [2].

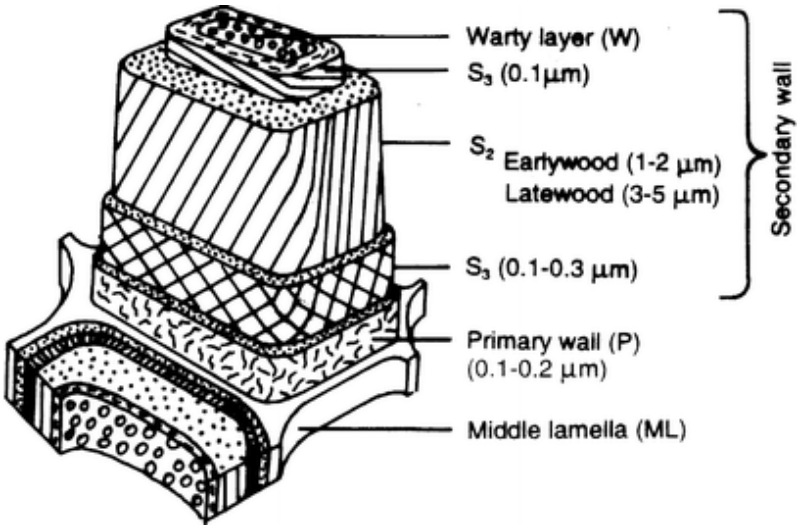

Figure 2.2: Hierarchical structure of a wood fibre [3].

2.1.2 Effect of moisture absorption on properties of wood fibers

Understanding how moisture absorption affects the mechanical characteristics of fibers at the cellular level is critical for using natural fibers in reinforcing composites. Changes in the environment have an impact on composites and their mechanical characteristics can vary significantly when temperature and moisture levels change.

Wood fibre structures are composed of cellulose fibres with several hydrophilic hydroxyl groups, meaning they are sensitive to moisture. This is a significant difficulty when it comes to wood fibres since it implies poor compatibility with most hydrophobic polymers. The rate water is absorbed by a composite is determined by several factors, including fibre type, matrix, temperature, water distribution within the composite, and water-matrix interaction, among other things. Therefore, wood fibre reinforced polymers can absorb a large quantity of water, resulting in a loss of mechanical characteristics. The chemical structure of the resin and crosslinking agent, as well as the temperature and relative humidity (RH), influence both the rate of water absorption and the overall quantity of moisture absorbed. [4]

In general, the strength and Young's modulus of wood decrease as the RH content rises. Moreover, different RH concentrations cause significant directional swelling and shrinking. Previous tensile studies on single wood fibres have shown that when the RH rises, the tensile stiffness of the fibre decreases [5].

2.1.3 Mechanical and physical properties of wood fibres

The usage of natural fibres in high-performance composites necessitates a thorough understanding of their mechanical properties. The tensile behaviour of natural fibres has been studied in a limited number of research studies. An examination of the literature reveals a significant gap in reported natural fibre tensile strength and

Young's modulus [6].

Understanding the mechanical reaction of wood fibres is critical for understanding and predicting the stability of living trees, as well as the behaviour of wood when used for production. Wood micromechanical data are key input parameters in applications such as the fabrication of fibre-based products, cardboard and paper, as well as assisting in efficient, economic, and sustainable use of this resource [6].

The surface property of wood fibres is one of the most important characteristics, it influences resin interfacial adhesion on the fibres surface as well as the mechanical properties of fibre-based composites. Fibre morphology, chemical composition, processing conditions and more, have an impact on this property. The fibres are less compatible with non-polar resin due to the strong polar nature of the surface. As a result, combining the intrinsic polar and hydrophilic properties of wood fibres with the non-polar properties of resins is challenging, resulting in poor stress transmission of composites under load. Using various physical and chemical surface treatments on fibres results in changes in the surface structure and changes in surface characteristics [1].

Wood fibres' mechanical properties are critical for their usage in the paper and composite industries. Materials' mechanical characteristics may be determined using two methods: macroscopic testing (for example tensile tests) and indentation tests. The macroscopic testing is used to determine the mechanical properties of the entire sample, whereas the indentation tests are used to determine the mechanical properties of a specific portion of the sample. Mechanical properties such as tensile strength, elongation, compressive strength, impact strength, and modulus are commonly obtained in macroscopic experiments. To present the mechanical performance of wood fibres, scientists generally utilize elongation, tensile strength, and Young's modulus [1].

Furthermore, due to variations in fibre diameter, the influence of clamping length, the measurement of elongation, and clamping effects, determining the tensile properties of fibres poses some additional challenges. It also depends on the tensile testing equipment, the methodology used to measure the fibres CSA, and the methodology used to compute Young's modulus. As a result, studying the tensile behaviour of natural fibres is not a simple task [6].

Below is a list of the different mechanical properties with a short description.

- Young's modulus, E: is a property of the material that indicates how easy it may stretch and deform. It is defined as the ratio of tensile stress to tensile strain.
- Tensile strength: is defined as the highest load a material can withstand without fracture when stretched, divided by the material's initial CSA.
- Tensile Stress: is the amount of force applied per unit area.
- Tensile Strain: is extension per unit length.

2.1.4 Environmental impact and recycled paper

It is commonly recognized that paper production, along with other types of industries, has significant environmental consequences. Both the use and handling of raw materials have several negative environmental effects. However, some new technologies can mitigate these effects, while also having economic benefits. One of these methods is recycling, which covers more than just the disposal of waste. When recycled, the fibres are exposed to a variety of mechanical, thermal and chemical effects and therefore, it has to be determined that they are not damaged severely and still provide good quality. As the pace of greenhouse gas emissions continues to rise and other health hazards concerns, scientists around the world have been enthusiastic regarding the research of environment-friendly materials [7].

Because of the economic and environmental benefits, paper product recycling has been conducted for a long time. Paper made from recycled fibres uses less energy, contributes to natural resource conservation, and minimizes pollution in the environment. Recent research initiatives for waste management system planning have focused on the conflict between economic optimization and environmental preservation [7].

On the other hand, recycled paper may have lower strength properties. Due to shorter fibre length, decreased intrinsic strength, and lower fibre-fibre bonding potential, cellulose fibres disintegrate during recycling. The chemical composition of wood fibres is critical for their recycling capability. When fibres are rewetted, their capacity to adjust the form and absorb water is diminished. As a result, fibre-fibre bonding is reduced, resulting in a reduction in paper strength [8].

2.1.5 ASTM Standard

American Society for Testing and Materials (ASTM) standards are utilized all throughout the world to improve product quality, increase safety, and make commerce easier [9]. For the tensile testing of natural fibre in this thesis, the closest applicable standard is ASTM C1557-20 the "Standard Test Method for Tensile Strength and Young's Modulus of Fibers". This ASTM standard covers from preparation, mounting, and testing of single fibres to determination the tensile strength and Young's modulus at ambient temperature [10]. This standard was used as a template when the experimental part was carried out.

2.2 Microscopes used in the thesis

This section will give a short description of the microscopes used throughout this project.

2.2.1 Scanning electron microscope

The scanning electron microscope (SEM) is a powerful and effective imaging tool. This instrument is used to scan the surface of a specimen with magnifications ranging from 100x to 100,000x, depending on the hardware used to create the electron beam, which includes electron gun and different lenses. To include the possibility of elemental analysis at the specimen surface, a SEM can also combine with an energy-dispersive spectroscopy. Backscattered electrons and secondary electrons, are two common signals for SEM imaging. The heart of the SEM, along with other components, is the electron gun. [11]

A focused ion beam (FIB) is generally combined with a SEM, making a combined FIB-SEM workstation. FIB is a scanning ion microscope, raster scanning the ion-beam across a sample surface and produces secondary electrons and secondary ions, which are collected for image generation. Additionally, the ion beam can sputter away materials. Thus, the FIB-SEM can be used to make high-quality cross-sectional cuts of materials normal to the sample surface to examine [12]. Figure 2.3 shows the SEM used in this thesis, a Leo 1550 field emission gun SEM by Zeiss. A field emission gun offers high resolution imaging.

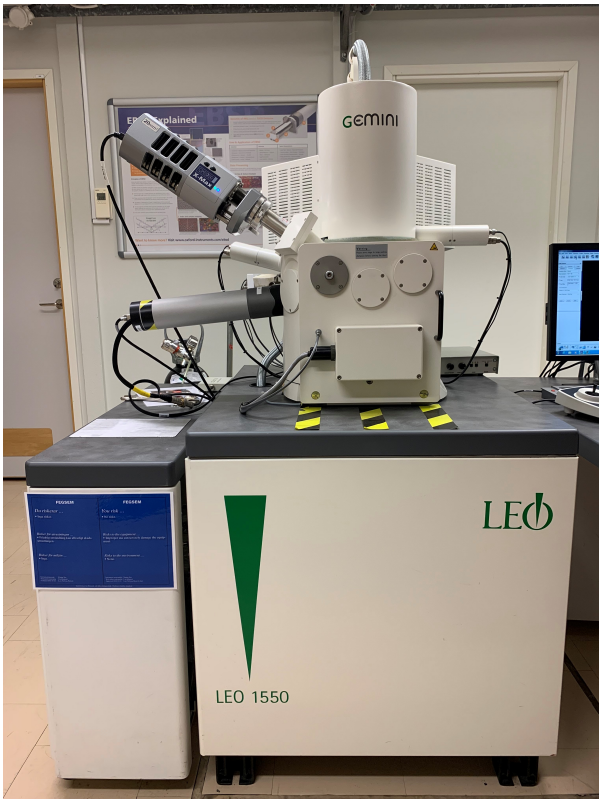

Figure 2.3: The SEM used in this thesis, a Leo 1550 field emission gun SEM by Zeiss.

2.2.2 Stereo microscope

In this project, the Stero microscope Discovery from ZEISS V20 was used, it is a motorized 20x zoom stereo microscope. This microscope was made with the goal of providing the best depth perception and zoom range possible. It is possible to go from the greatest overview to the tiniest details by using the 20:1 zoom range. All the optical components work together to create stunning 3D visuals with outstanding depth awareness. Magnification, focus, contrast, brightness, and other can be adjusted with this stereo microscope [13]. Figure 2.4 shows the stereo microscope used in this thesis.

Figure 2.4: The stereo microscope used in this thesis.

2.3 Young´s modulus

A materials stress-strain curve illustrates the relationship between stress and strain. It is calculated by progressively adding load to a test specimen and monitoring deformation, from which stress and strain may be calculated. Many characteristics of a material are revealed by these curves, including the Young's modulus, yield strength, and ultimate tensile strength.

To calculate the ultimate tensile strength of the specimen, Equation (2.1) is used

$$\sigma = \frac{F}{A} \tag{2.1}$$

where σ is the ultimate tensile stress, F is the load at failure [N] and A is the CSA of the specimen [mm^2].

The strain of the specimen is calculated with the help of Equation (2.2)

$$\varepsilon = \frac{\delta}{L} \tag{2.2}$$

where ε is the strain, δ is the elongation and L is the gauge length of the specimen [mm].

Young´s modulus is a mechanical property that determines the tensile or compressive stiffness of the fibre when the force is applied lengthwise. The change in size of a specimen constructed of an isotropic elastic material under tensile or compression stresses may be calculated using Young's modulus. It can, for example, determine how much a material sample expands or shortens under tension or compression. The Young´s modulus is the relation between stress and strain and is calculated as Equation (2.3)

$$E = \frac{\sigma}{\varepsilon} \tag{2.3}$$

where E is the young's modulus [Pa].

2.4 Weibull statistics

The use of Weibull statistics to describe fibre strength is quite popular among material scientists. Nevertheless, while the weakest link model appears to be highly appealing from a physical perspective, the mathematics involved in all circumstances is not so simple [14]. The Weibull distribution is usually used to model mechanical properties that are widely dispersed and to measure the variation of the strength of natural fibres [15]. In order to apply Weibull statistics, certain requirements must be met. It is important to consider the brittleness of the material, as well as the assumption that the strength depends on critical flaws in the material [14].

Weibull statistics were used in this thesis to understand the strength and possible defects in the microstructure of the tested fibres. Equation 2.4 was used to calculate the Weibull statistics.

$$\ln\left(\ln\left(\frac{1}{1-P}\right)\right) = m\ln(\sigma) - m\ln(\sigma_0) + \ln(L) \tag{2.4}$$

where L is the gauge length of the fibre, σ is applied strength, σ_0 is the characteristic strength and m was the Weibull modulus. To get P, Equation 2.5 is used

$$P = \frac{i - 0.5}{n} \tag{2.5}$$

where P is the probability index, n is the number of data points and i is the rank of the i:th data point. To get the characteristic strength, σ_0, Equation 2.4, is rearranged where m, σ_0 and L is characteristics values for the fibre, L and σ is known values.

$$M = \ln L - m\ln\sigma_0 \rightarrow \ln\sigma_0 = \frac{1}{m}(\ln L - M) \rightarrow \sigma_0 = e^{\frac{\ln L - M}{m}} \tag{2.6}$$

The root mean square deviation (RMSD) is a common method of calculating a model's residuals (errors) in predicting quantitative data. How far away the data points are from the regression line is a measure of the residuals. RMSD is a measure of how spread out these residuals are. That is, it indicates how near the data is clustered around the line of best fit. To calculate the Root-mean-square deviation, Equation 2.7 were used.

$$\text{RMSD} = \sqrt{\left(\sum_{i=1}^{n} \frac{(\hat{y}_i - y_i)^2}{n}\right)} \tag{2.7}$$

where, $\hat{y}_i$ are predicted values, y_i are observed values and n is the number of observations.

Normalization Root-mean-square deviation (NRMSD) was calculated to get the residual variance. To calculate the NRMSD deviation, Equation 2.8 was used

$$\text{NRMSD} = \frac{\text{RMSD}}{y_(\text{max}) - y_(\text{min})} \tag{2.8}$$

3
Method

This experimental study was performed at Chalmers University of Technology. The purpose of this chapter is to explain the methodology behind the obtained results. The purpose is to make it possible for all readers of this chapter to reproduce the results obtained in this thesis and to use this method as a template for further research in this area.

In the first section of this chapter, the literature study will be presented, section 3.1, followed by a description of specimen preparation in section 3.2. In section 3.3, testing at different relative humidity levels are explained, after which the equipment utilized in this thesis are presented, section 3.4. Last, in section 3.5 the method used to get the CSA is described.

3.1 Literature study

The literature study was carried out by searching for and reading relevant books, e-books and articles about the topic of single wood fibres. Most of the online sources were found through Chalmers University of Technology online library service and in databases like:

- ProQuest platform.
- ScienceDirect.
- Knovel.

Key words that were used during the literature study were among others; *Single wood fibres*, *Tensile test*, *Weibull statistics*, *Micromechanical testing*, *Mechanical properties*, *Moisture*, *Relative humidity*, *Cross-sectional area*, *Environmental impact*, *In-situ test*.

Relevant information was also covered through reliable websites.

3.2 Specimen preparation

This section describers how the sample preparation were carried out. The collection of fibres were prepared as described in subsection 3.2.1 followed by a description of how the single fibres were prepared in subsection 3.2.2. How the fibres were sorted are presented in subsection 3.2.3 after which the aluminum frame used for the tensile tests is described in subsection 3.2.4, and last, the method to determine the gauge length of the fibres is presented in subsection 3.2.5.

3.2.1 Collecting fibres

The fibres investigated in this thesis are wood fibres provided by Tetra Pak. With the help of two pair of tweezers, fibres from mesh 14, which is a fibre cake, were collected and placed on a small plate, see Figure 3.1. The plate was then weighed on a very sensitive scale seen in Figure 3.2. Distilled water was measured in a beaker to 20 ml and thereafter the fibres were placed in the water in the beaker. A piece of aluminium was placed on top of the beaker to prevent any water vapour to escape, and then the beaker was placed in an ultrasonic agitation (Branson 1510 ultrasonic cleaner), see Figure 3.3. The beaker would stay in the ultrasonic cleaner for 1,5 hours before being taken out to make the fibres break free. The fibres used in this project were kept in the water for a maximum of 3 weeks. After this, new fibres were collected in the same way as described before and used instead.

Figure 3.1: Fibre cake of mesh 14 from Tetra Pak to the left and collected fibres on the plate to the right.

Figure 3.2: Sensitive scale used to weigh the fibres.

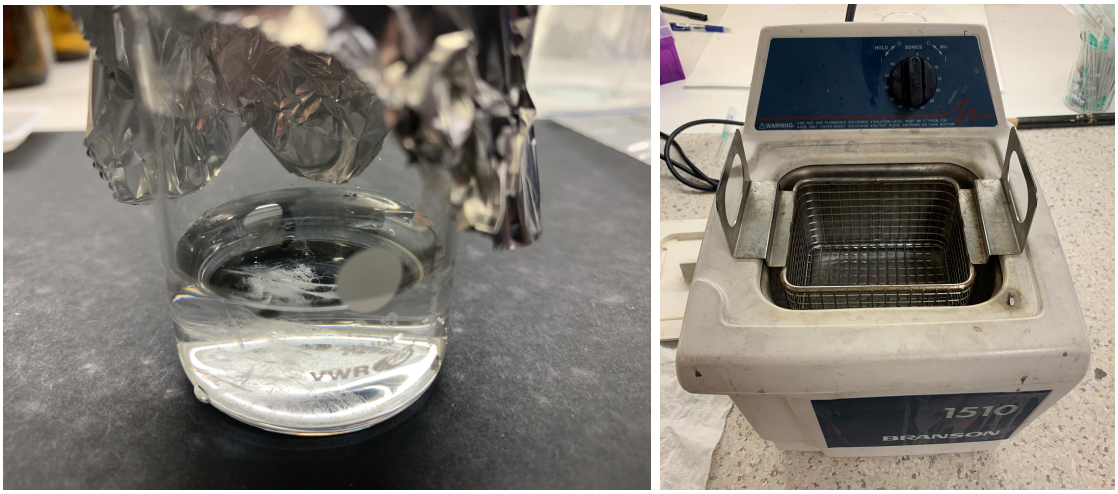

Figure 3.3: The beaker containing water and fibres with aluminum on top is shown to the left and the ultrasonic agitation is shown to the right.

3.2.2 Separating the single fibres

Two equal pieces of Kapton were cut with a pair of scissors and one of the pieces was placed on a glass plate. With a pair of tweezers, a lump of fibres was taken out of the beaker. And with the help of another pair of tweezers, single fibres were pulled out from the lump, see Figure 3.4. The fibres were placed as straight as possible on the Kapton as shown to the top picture in Figure 3.5. When the collection of the fibres was done, the other piece of Kapton was placed on top of the fibres and on top of that, another glass plate was placed. The Kapton is used to prevent the fibres to stick on the glass plates and to make sure that the glass and the Kapton

would stay in place and not move, two rubber bands were placed around the glass plates, see the bottom picture in Figure 3.5.

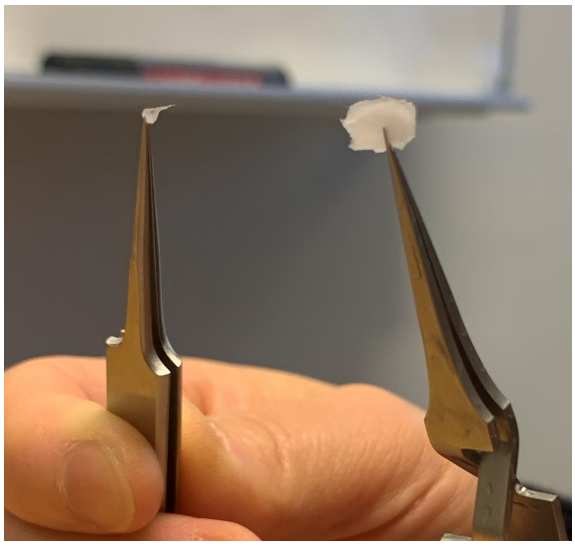

Figure 3.4: Collecting fibres from a lump of fibres that has been in water.

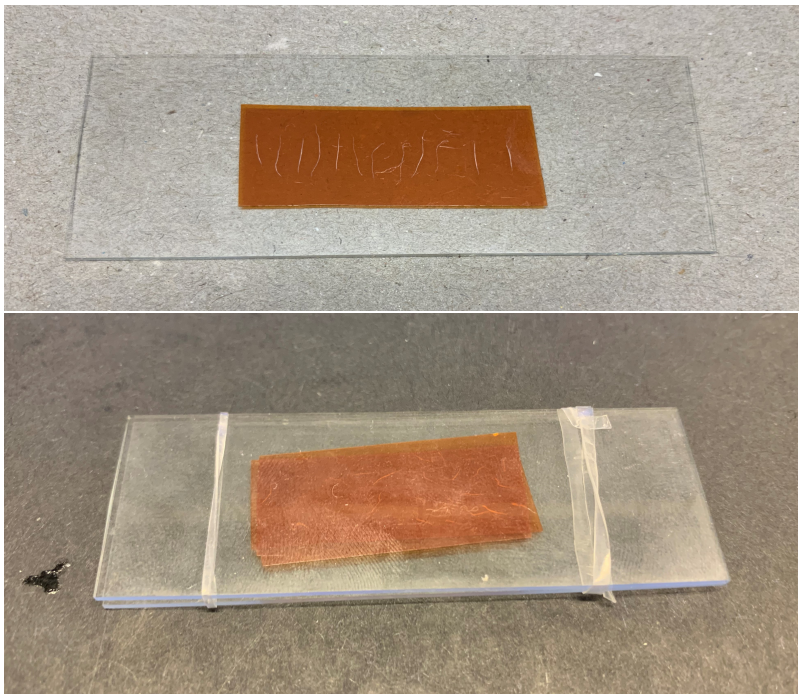

Figure 3.5: The figure at the top illustrates how the fibres are lined up on the Kapton and how the rubber bands are placed to keep the glass plates together is shown in the figure at the bottom.

3.2.3 Fibre selection

A few days after the preparation of fibres, the rubber bands, the top glass and Kapton were removed. The glass plate with the remaining Kapton with the fibres on was

placed under a stereo microscope (Zeiss Stereo Discovery.V20 Stereo Microscope). Pictures were taken on the fibres with 7,5x and 30x magnifications and all the fibres were measured. Fibres that were spun, bent, contained more than one fibre or had other defects were in this step discarded.

3.2.4 Aluminum frame

A frame of aluminum foil was designed, see Figure 3.6, to be easily fixed onto the tensile device to carry out the tensile test on single fibres. The frames dimensions are 43 mm long, 5 mm wide and 0.009 mm thick. One drop of super glue was placed on both sides of the hole of the aluminium frame. A fibre was then taken from the Kapton with the help of a pair of tweezers and placed in the middle of the hole of the frame with the ends in the glue. The pair of tweezers was also used to adjust the fibres so they would be as straight as possible. The aluminum frame was stored in a box until the glue had dried. Figure 3.7 shows the aluminum frame where the fibre has just been glued on.

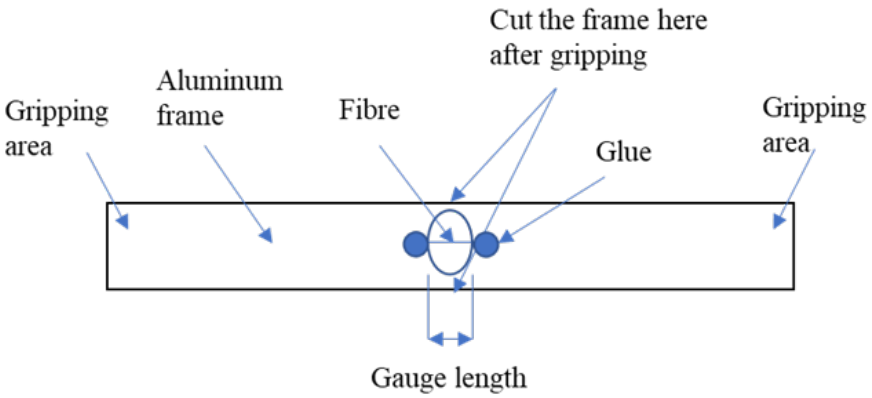

Figure 3.6: Aluminum frame for single fibre specimen for axial tensile testing.

Figure 3.7: Illustration of an aluminum frame with the fibre glued on.

3.2.5 Gauge length

When the glue had dried, the aluminium frame was placed under the stereo microscope again and pre-failure gauge length observation was conducted on every test

specimen. The fibre was photographed, and the gauge length was measured according to Figure 3.8. If the fibres were bent, twisted or had any other error, they were discarded. After the gauge length had been measured, the test samples were ready for testing.

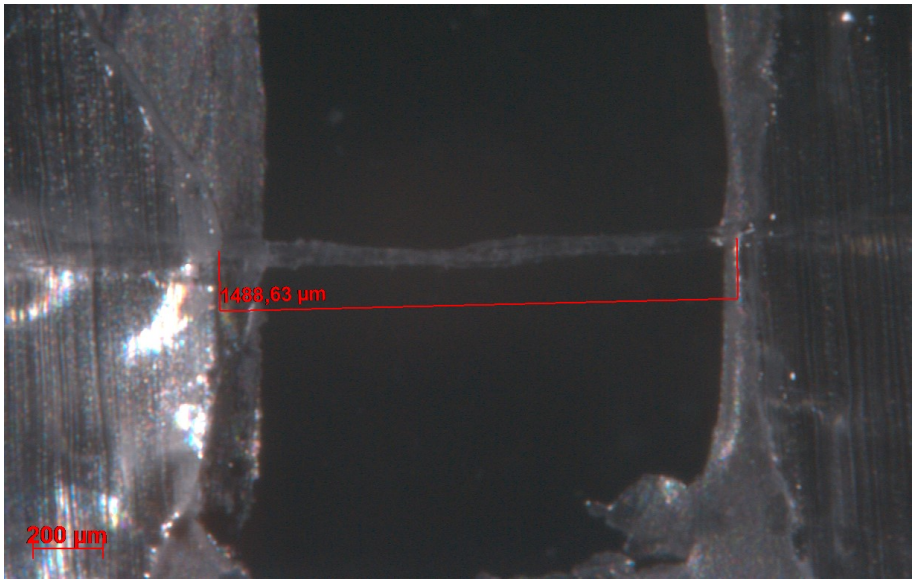

Figure 3.8: Gauge length photographed and measured with the help of a stereo microscope.

3.3 Conditioning of fibres of different relative humidities

In this section, the methods used to condition the fibres with 0% RH, 50% RH as well as 100% RH are described.

3.3.1 0% relative humidity

Test samples were placed on a glass plate, see Figure 3.9 and then placed inside an oven. The oven was set to 60 degrees Celsius to make sure that the glue would not melt, and the test samples stayed in the oven for 72 hours. After 72 hours, the test samples were taken out of the oven and directly placed in a desiccator, see Figure 3.10, to protect them from contacting water vapor and preserve the dry climate. One test sample at a time was taken out from the desiccator and the tensile test was immediately carried out.

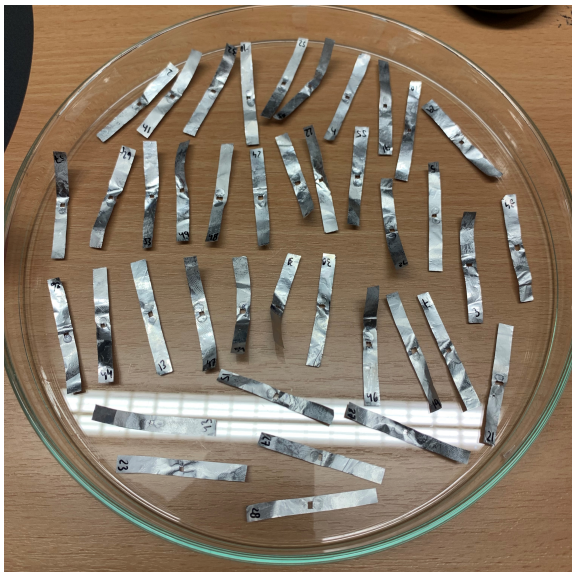

Figure 3.9: Illustration of the test samples lined up on the glass plate before placed in the oven.

Figure 3.10: Illustration of the desiccator used throughout this thesis.

3.3.2 50% relative humidity

Test samples were placed in a plastic box and then put in a climate chamber with 50% RH and 20 degrees Celsius with the lid off. After 72 hours in the climate chamber, the lid on the plastic box was sealed and the box was placed in an air-tight plastic bag, see Figure 3.11, before it was taken out of the climate chamber. The test samples were then placed in the desiccator and one test sample at a time was taken out from it and the tensile test was immediately carried out.

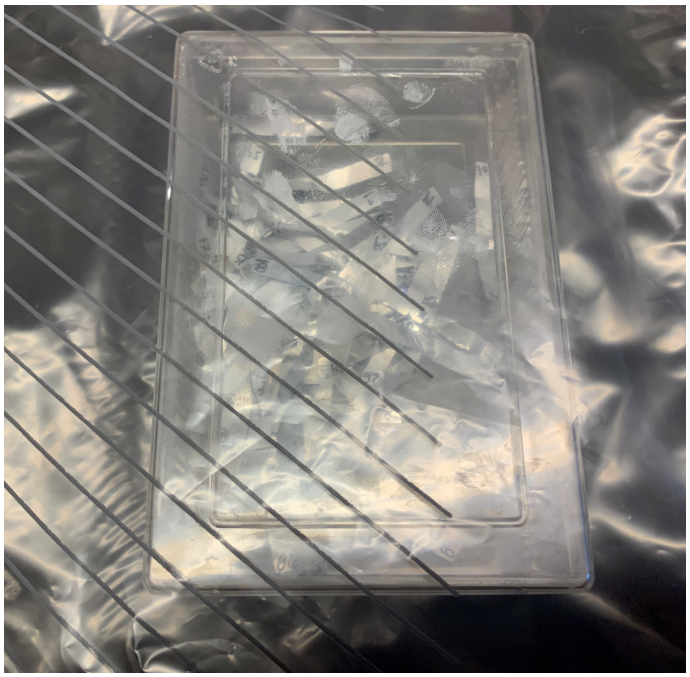

Figure 3.11: Photograph of the test samples in the box in the air-tight plastic bag before the tensile test.

3.3.3 100% relative humidity

Distilled water was poured into a glass box and four small glass beakers were filled with water. These glass beakers were then put into the glass box at each corner. A metal mesh was then placed on top of the glass beakers which are used to hold up the mesh a few millimeters over the water. Test samples were placed on top of the mesh as shown in Figure 3.12, and the airtight lid was put on, see Figure 3.13. The box was stored at room temperature for one week. After this week, one test sample at a time was taken out from the glass box the tensile test was immediately carried out.

Figure 3.12: Photograph of the test samples on the metal mesh in the box.

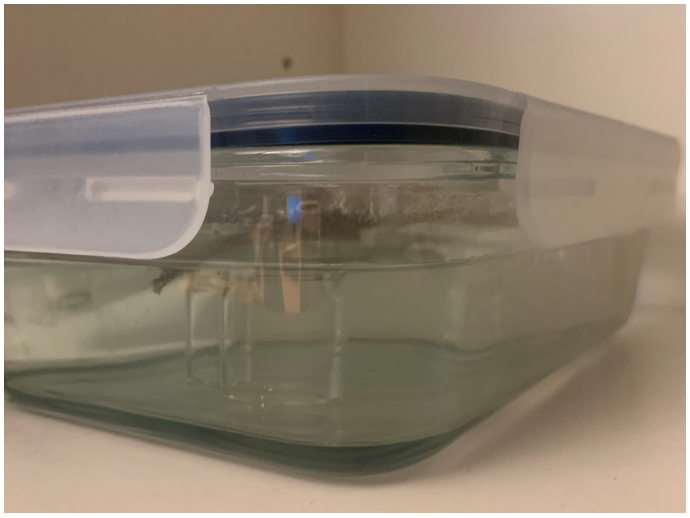

Figure 3.13: Illustration of the test samples in the closed box.

3.4 Single fibre tensile testing

This section describes the tensile test machine in subsection 3.4.1 as well as the method used to perform the tensile tests. Determination of system compliance is described in subsection 3.4.2.

3.4.1 Tensile test machine

The Kammrath and Weiss Materials Testing Modules were used in this thesis to carry out the tensile tests. PC-controlled microprocessor hardware (DDS4) and a software package (MDS) was used to collect data from the tensile tests. Online

recording of the displacement, force and time is used to collect data. This testing equipment is compatible with the majority of today's SEM specimen stages [16].

The tensile tests were conducted by using the tensile machine under a constant speed of displacement of 5 μm/s at room temperature. The tensile machine was plugged into the outlet and connected to a computer. On the computer, the program called MDS was started and the tensile machine and the program were connected. The aluminium frame was placed in the tensile machine as illustrated in Figure 3.14. Before the test could start, the aluminum frame was cut on the sides next to the fibre so that the frame was only connected through the fibre, see Figure 3.15. During the tensile test, time, displacement and force were monitored simultaneously as well as recorded with the help of the program MDS. When the test was done, e.g., after the fibre had been pulled apart, the aluminium frame was saved for analysing the cross-section, and all the documentation was stored.

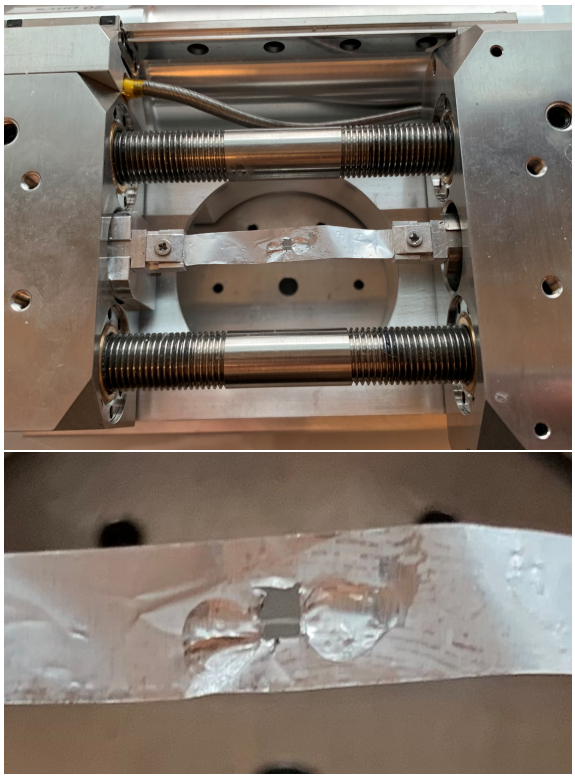

Figure 3.14: The photograph on the top shows the test sample placed in the tensile machine before the cut and the bottom photograph shows the frame and fibre up close.

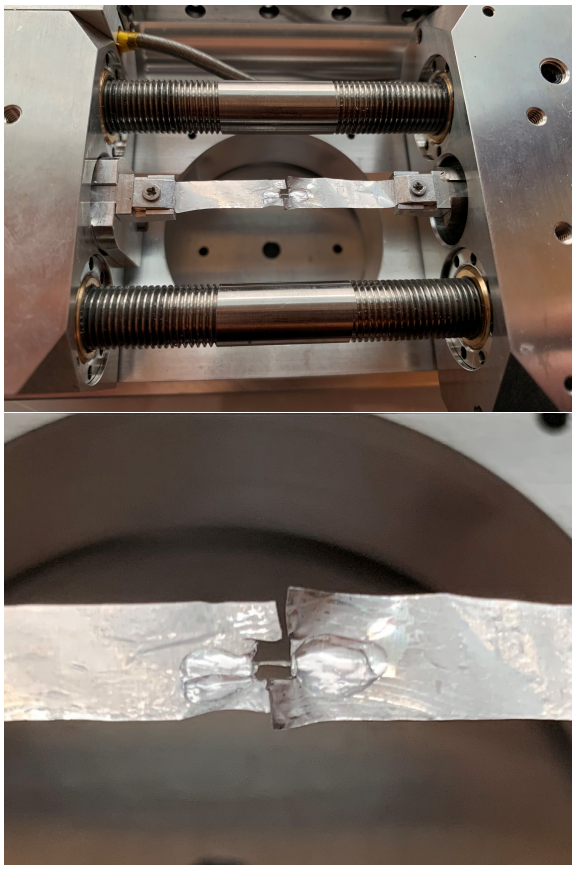

Figure 3.15: The photograph on the top shows the test sample placed in the tensile machine after the cut and the bottom photograph shows the frame and fibre up close.

3.4.2 Determination of System Compliance

Before the tensile test, the machine was calibrated, and the system compliance was determined. The machines compliance can affect the calculated result, therefore the system compliance is determined to know how big this effect is.

Test samples of various gauge lengths of roughly 2, 5, 10, and 15 mm were made in the same way as stated in section 3.2, with the exception that carbon fibres were used to allow testing of various gauge lengths and tested as described in section 3.4.

A plot of (ΔL/F) versus (l_0/A) makes a straight line with a constant slope of (1/E). ΔL is the recorded displacement provided by the tensile machine, F is the force, l_0 is the gauge length of the fibre and A is the CSA of the fibre. The system compliance can be read of where the line crosses the y-axes, this is how C_s is measured.

The obtained C_s value is used in Equation 3.1 to get the actual elongation of the specimen.

$$\Delta l = \Delta L - C_s F \tag{3.1}$$

where Δl is the actual elongation of the specimen [m], ΔL is the recorded displacement provided by the tensile machine, C_s is the system compliance [m/N] and F is the force [N].

3.5 Determination of single fibre cross-sectional area

The saved fractured samples were now used. The fibre was cut from the aluminum frame and placed as straight as possible on a copper tape. A layer of silver glue was then placed on top of the fibre as shown in Figure 3.16.

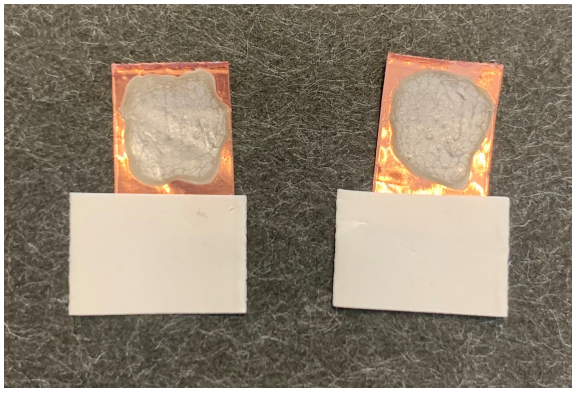

Figure 3.16: Photograph of copper tape with the fibres lined up and silver glue placed on top.

When the glue had dried, a cut was made through the glue, fibre and copper tape with the help of a scalpel. When this was made for all the fibres, the copper tape with the fibres were glued on a small piece of copper. This was done to analyse several fibres at the same time in the SEM without frequently vent and pump the SEM. The copper piece was then placed in the SEM where images were taken to later be used to determine the cross-sectional area (CSA). A program called ImageJ was used to measure the CSA of the fibres. ImageJ is free software that may be used to analyze scientific photographs. In this thesis, it was used to obtain the CSA of the fibres. The SEM image was opened in ImageJ as illustrated in the top picture in Figure 3.17. In the image, a scale bar is shown. This was used to calibrate the program, after which it could be used to calculate the area of any drawn shape (like the bottom piture shows in Figure 3.17). This was how the CSA were obtained for all the fibres in this thesis. Unfortunately, not all fibres gave a good cross-section image and was therefore discarded and not used in the results.

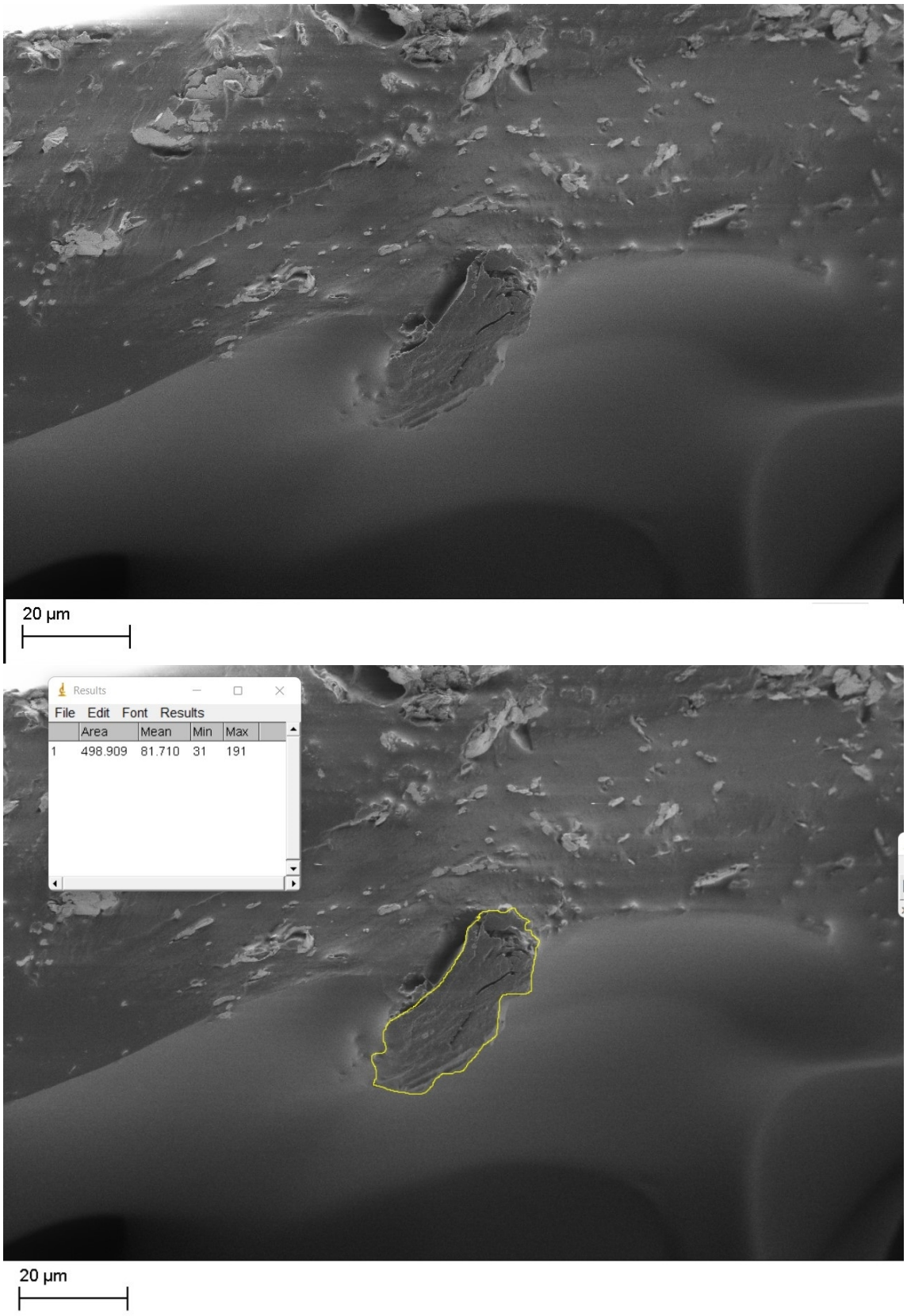

Figure 3.17: SEM photograph of a fibres cross-section in the top picture and in the bottom picture an photograph of how ImageJ was used to obtain the CSA of the fibre.

4

Results

A robust and high throughput method has been developed to conduct tensile tests on individual single wood fibres. By using this method, the impact of different humidity conditions on the mechanical properties of single wood fibres was investigated. Weibull statistics was carried out to understand the strength and possible defect in the microstructure of the material.

The results from the determination of system compliance is presented in section 4.1 and the stress-strain curves are presented in section 4.2, after which the Young´s modulus results is shown in section 4.3. The obtained results from the Weibull statistics is shown in section 4.4. The discussion regarding the results is presented in section 5.

4.1 System compliance

The average diameter of the commercial carbon fibres was 5μm and in Table A.1 in Appendix A, all fibres gauge lengths can be found. With the help of the recorded displacement and force, the slope of the curves could be calculated, see Figure 4.1. Figure 4.2 shows a plot of (ΔL/F) versus (l_0/A) which makes a straight line with constant slope of (1/E). The system compliance could be read of where the line crosses the y-axes, which in this case was 0.0011 [m/N].

To show how the system compliance influence the results obtained by the tensile test, Figure 4.3 has been made. This figure shows a force-displacement graph over one fibre from each humidity test, which are shown with the colored lines. The actual elongation of these fibers are shown with the black dashed, dotted and dash-dotted lines but with a 0.01 N offset to distinguish the curves. Since the value for system compliance is so small, 0.0011 [m/N], the impact the tensile machine has on the result of the tensile tests was found to be negligible. Hence, the recorded values for displacement were used rather than the actual elongation.

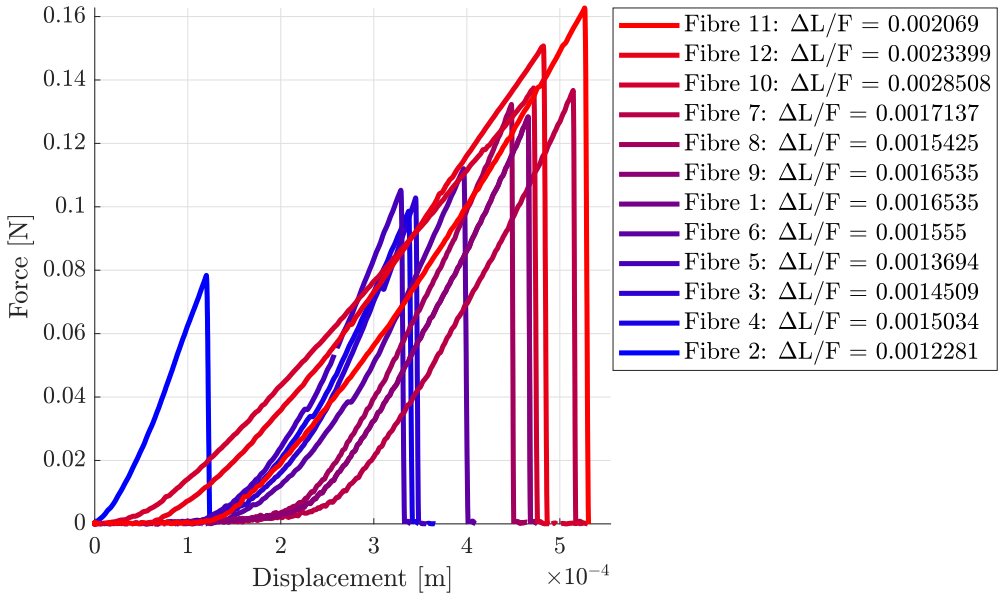

Figure 4.1: Illustration of force-displaccement curve of the carbon fibres.

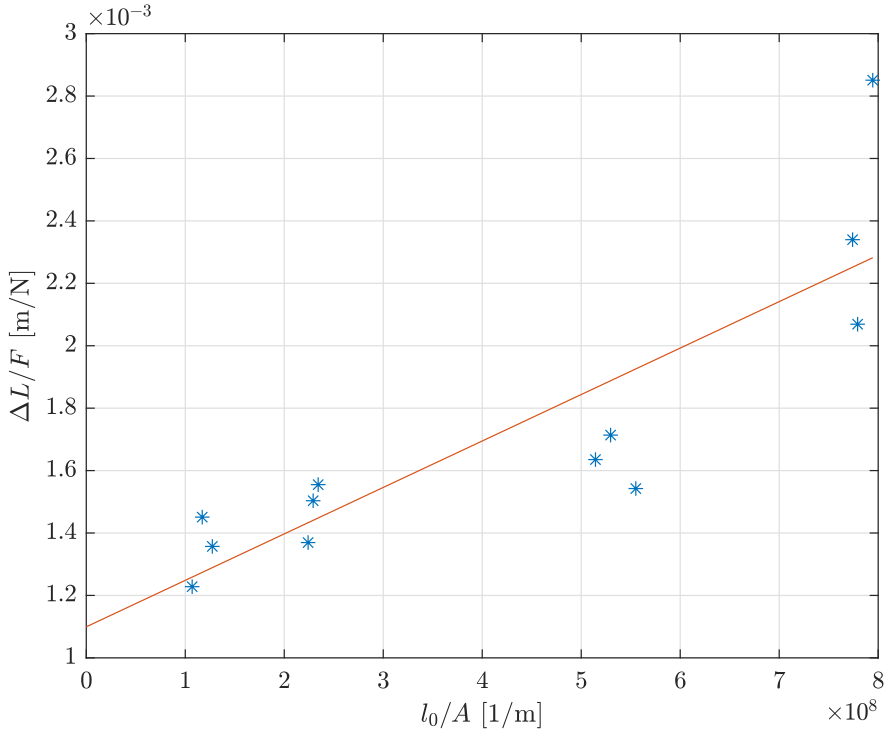

Figure 4.2: Illustration of (ΔL/F) versus (l_0/A) which makes a straight line with constant slope of (1/E).

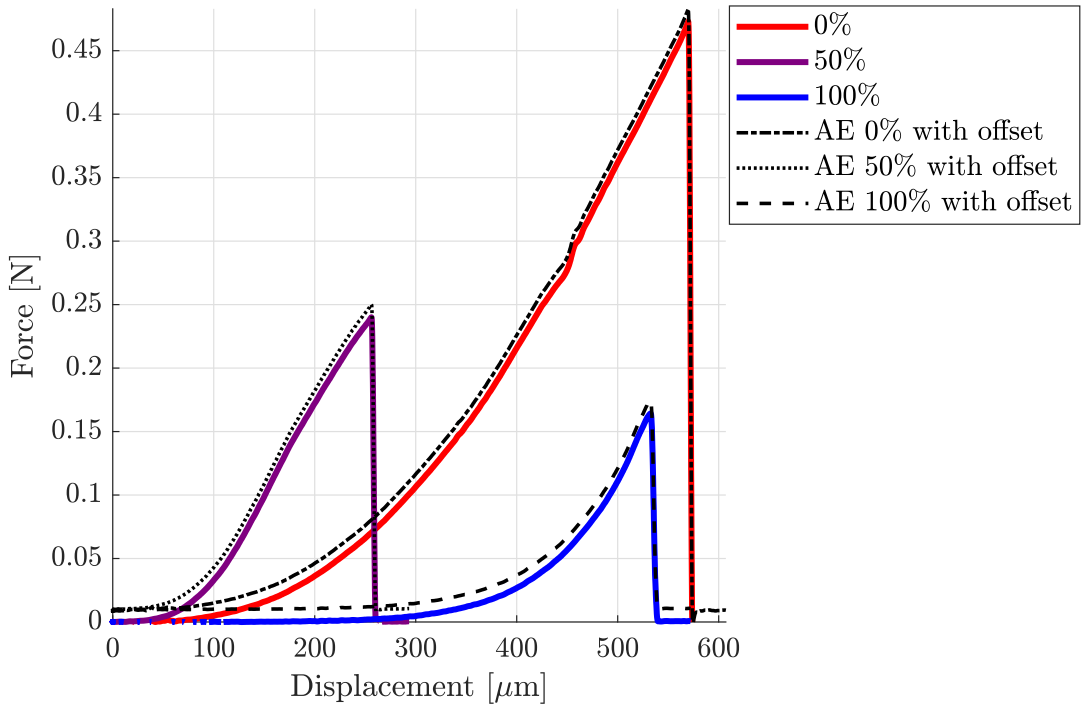

Figure 4.3: Force-displacement graph over one fibre from each RH, which are shown with the colored lines. The actual elongation of the same fibers are shown with the black dashed, dotted and dash-dotted lines but with a 0.01 N offset to distinguish the curves.

4.2 Stress-strain curves

The results from the tensile tests in different humidity environments are presented in this section.

For the three different humidities, result from 22 fibres were obtained. For each humidity, two graphs with result from 11 fibres ranking from the highest stress value to the lowest in each graphs were made to make it easier to analyse the result. In each graph, the more red the lines are the higher the stress, and the bluer the lines are, the lower the stress. This was made in both graphs for the same RH. It´s important to notice that the colors of the lines are representative to that specific graph and cannot be compared to the other graphs. So, if a figure has a red line, it do not mean that the value of the stress is higher than a blue line in another graph. Figure 4.4 illustrates the result from the tensile test with 0% RH, Figure 4.5 illustrates the result from the tensile test with 50% RH and Figure 4.6 shows the result from the tensile test with 100% RH.

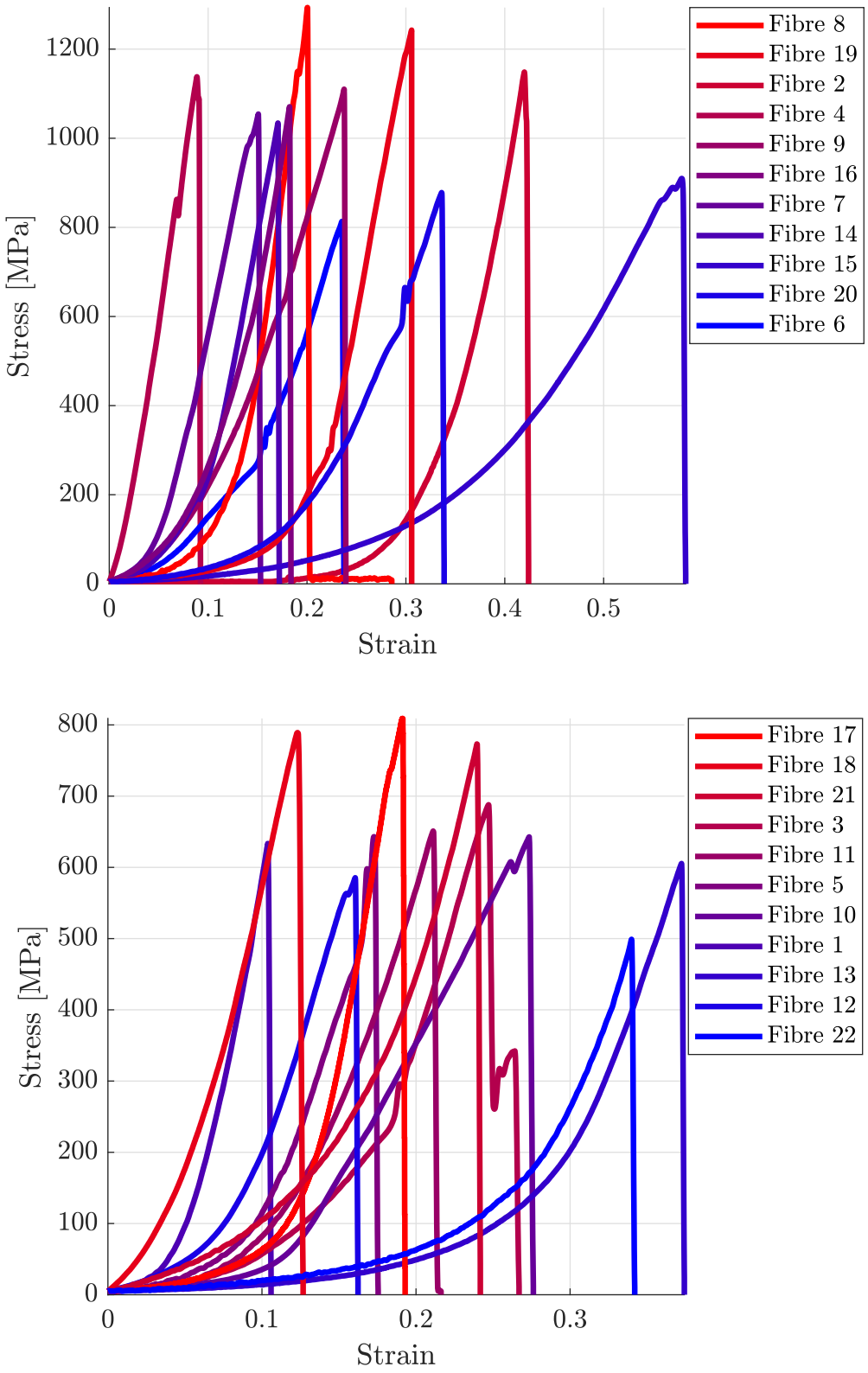

Figure 4.4: Stress-strain curves of the tensile tests from 0% RH. The figure on the top shows the 11 fibres with the highest stress value and the one at the bottom the 11 fibres with the lowest stress value.

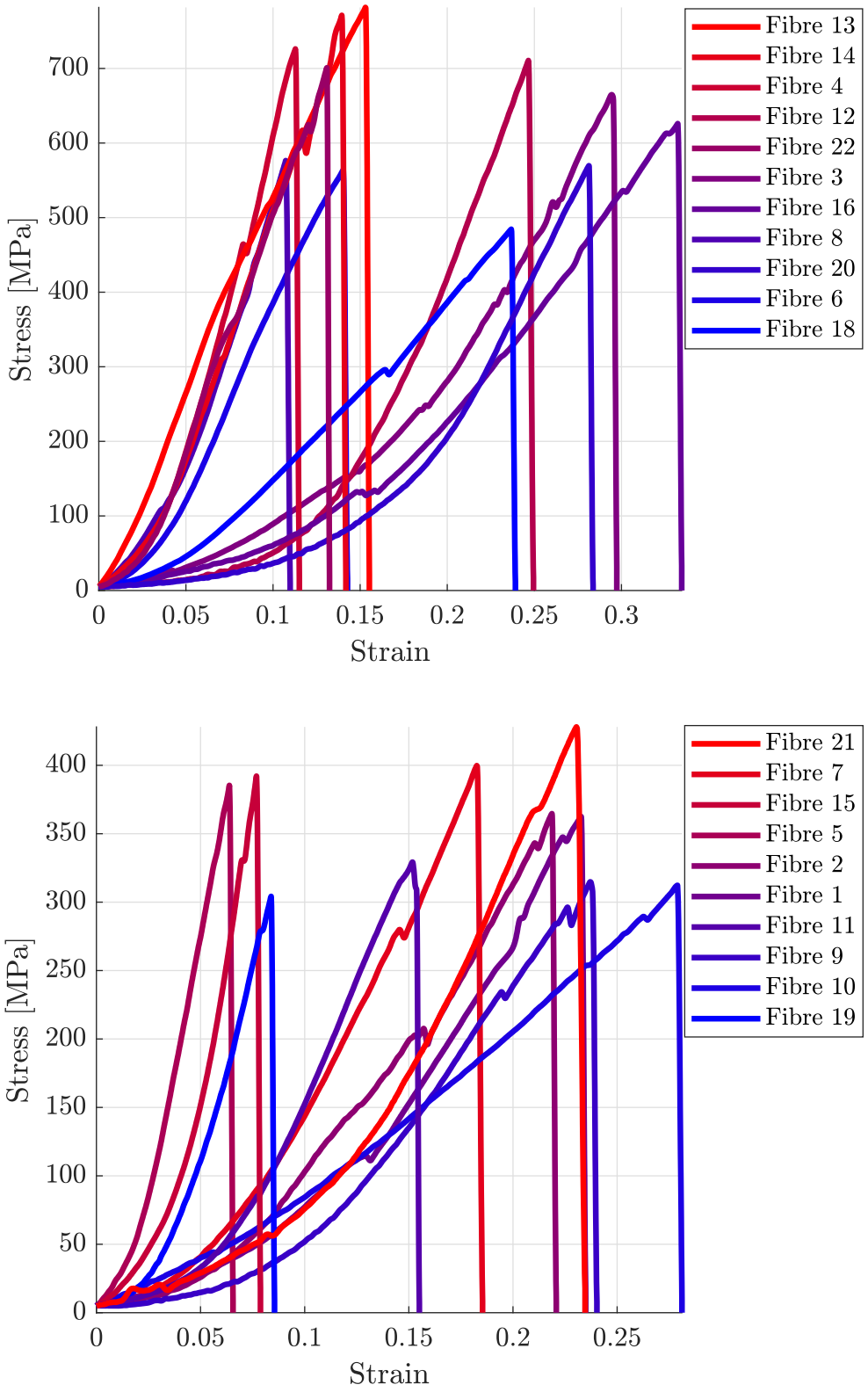

Figure 4.5: Stress-strain curves of the tensile tests from 50% RH. The figure on the top shows the 11 fibres with the highest stress value and the one at the bottom the 11 fibres with the lowest stress value.

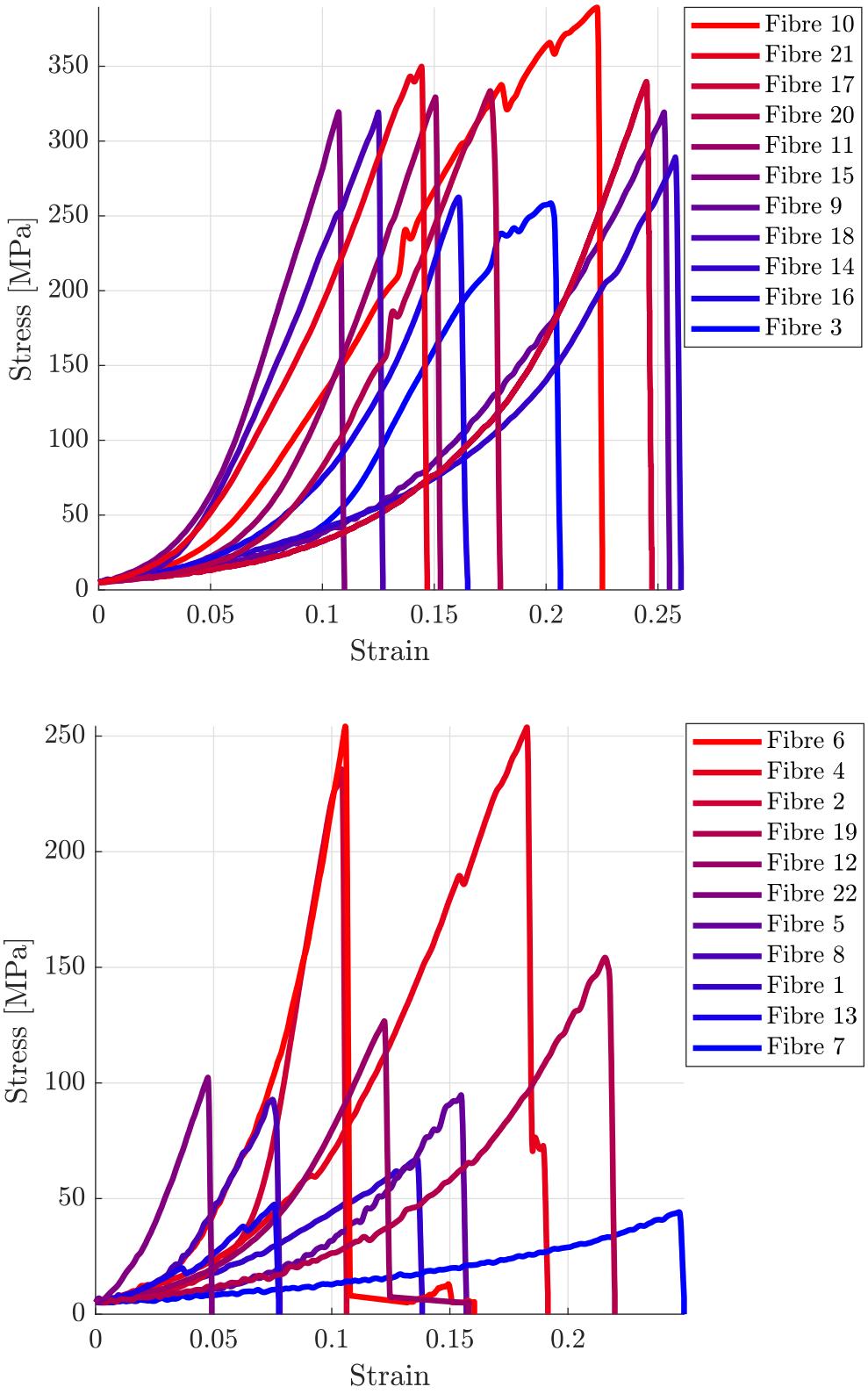

Figure 4.6: Stress-strain curves of the tensile tests from 100% RH. The figure on the top shows the 11 fibres with the highest stress value and the one at the bottom the 11 fibres with the lowest stress value.

In Table 4.1, measured ultimate tensile strength (UTS), standard deviation and average values for the different RH experiments can be found. In Table A.2 to A.4 in Appendix A, the UTS values for each fibre are presented.
It can be seen when analysing the stress-strain curves that 0% RH has the highest UTS and 100% RH has the lowest. This can also be seen in Table 4.1. The UTS for 0% RH is between 499 and 1293 MPa with an average value of 864. For the 50% RH test, the UTS is between 304 and 782 MPa and the average is 506. The UTS for 100% RH is between 44 and 389 MPa and the average is 227. The standard deviation is highest at 0% RH while lowest at 100% RH.

Table 4.1: Calculated ultimate tensile strength, standard deviation and average values for the different RH experiments.

Experiment:	**UTS:**	**Standard deviation:**	**Average:**
0%	499-1293	237	864
50%	304-782	166	506
100%	44-389	113	227

4.3 Young´s modulus

Figure 4.7 to 4.9 illustrates how the slops differs, the strain is therefore not correct. To see the correct value for the strain for the fibres, see Figure 4.4 to 4.6. The lines are steeper the more red they are, hence, a higher young´s modulus value.

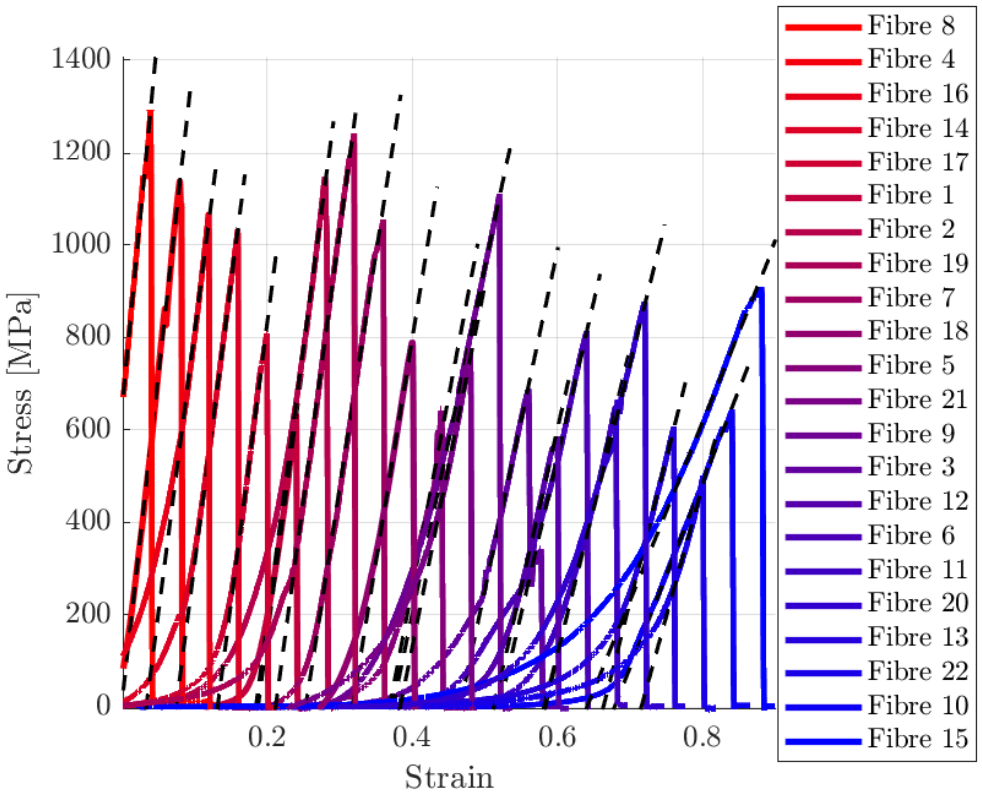

Figure 4.7: Illustration of the slope for the fibres form 0% RH.

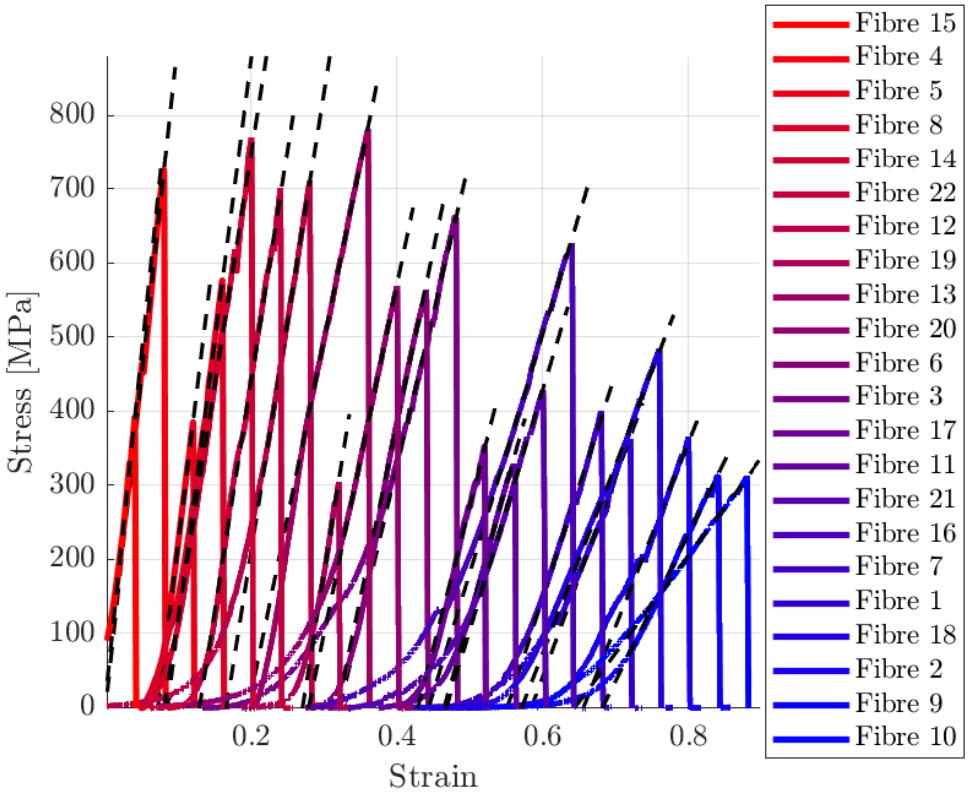

Figure 4.8: Illustration of the slope for the fibres form 50% RH.

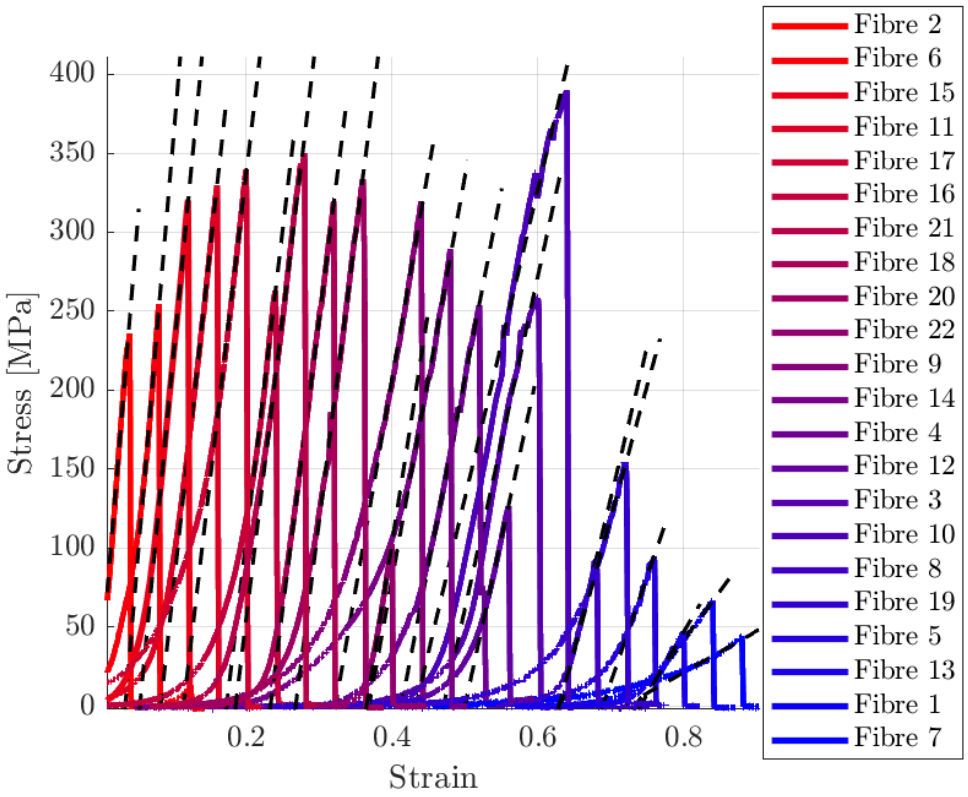

Figure 4.9: Illustration of the slope for the fibres form 100% RH.

In Table 4.2, calculated Young´s modulus, standard deviation and average values for the different RH experiments can be found. In Table A.2 to A.4 in Appendix A, the Young´s modulus values for each fibre are presented.

Table 4.2: Calculated Young´s modulus, standard deviation and average values for the different RH experiments.

Experiment:	Young´s modulus [GPa]:	Standard deviation:	Average:
0%	3.88-16.41	3.36	9.08
50%	1.31-9.41	2.31	4.78
100%	0.26-5.62	1.50	2.83

It can be seen when looking at Figure 4.7 to 4.9, that there is almost a tendency that with a higher max value of stress of the fibre, the steeper the slope. From Table 4.2, it can be seen that the Young´s modulus is between 3.88 and 16.42 GPa for 0% RH test with a average of 9.08. For the 50% RH test, the Young´s modulus is between 1.31 and 9.41 GPa and the average is 4.78. The Young´s modulus is between 0.26 and 5.62 GPa and the average is 2.83 for the 100% RH test. The standard deviation is lowest for 100% RH and highest for 0% RH.

4.4 Weibull statistics

Figure 4.10 shows the Weibull statistics graph over the different humidity experiments, where the red line represents the 0% RH tests, the green line the 50% RH tests and the black one the 100% RH tests.

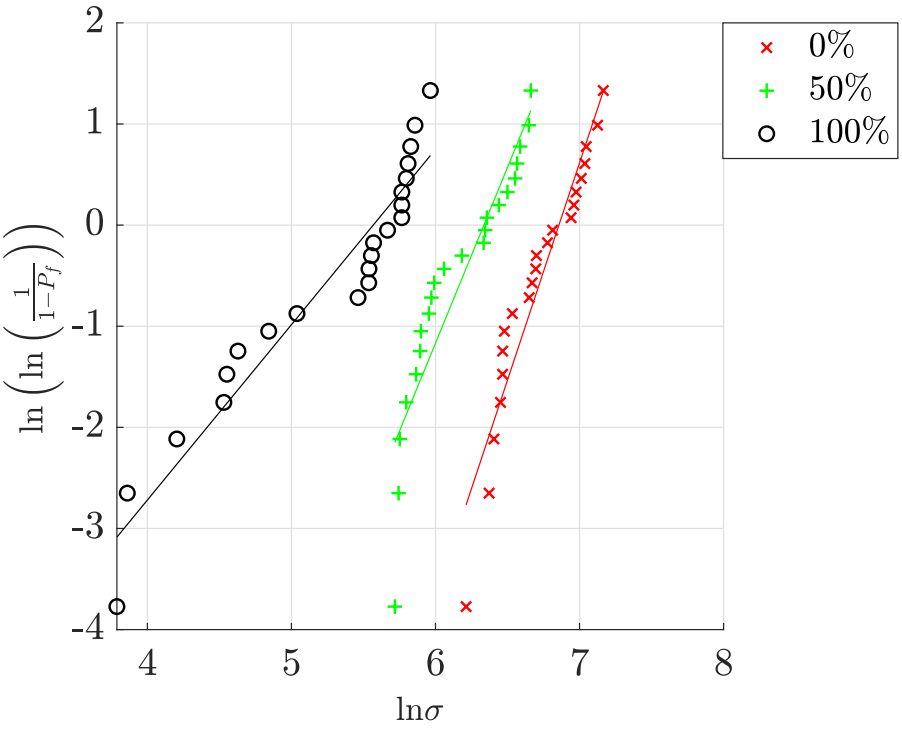

Figure 4.10: Illustration of Weibull statistics graph over the different humidity experiments.

In Table 4.3 the collected data from Figure 4.10 is presented, which includes the lines equations, Weibull modulus and characteristics value from the different experiments. The NRMSD value obtained from Equation 2.7 is also presented in this table.

Table 4.3: Data obtained from Figure 4.10 as well as Equation 2.7.

Experiment:	**y:**	**m:**	**NRMSD:**	σ_0**:**
0%	4.29x-29.44	4.29	0.0699	1092
50%	3.48x-22.03	3.48	0.0923	660
100%	1.73x-9.66	1.73	0.0680	351

It can be seen from Table 4.3 that 0% RH yielded the highest value for m, while 100% RH yielded the lowest. From the Table, it can also be seen that 0% RH provided the highest value for the characteristics strength and 100% RH the lowest. For NRMSD, 100% RH had the lowest NRMSD value (i.e., the highest degree of linearity) while 50% RH had the highest value. It is also noteworthy that the value

of NRMDS for all the experiments is very close to 0, indicating a good degree of linearity.

5
Discussion

In this chapter, the result presented in chapter 4 is discussed in section 5.1 and 5.2 followed by some uncertainties in section 5.3. Developments of the method is presented in section 5.4, then future development is discussed in section 5.5.

5.1 Stress-strain curves and Young´s modulus

Generally, from observing the graph, it can be said that moisture plays a significant role in influencing the mechanical properties of the fibers.

The test with the highest UTS was the 0% RH and 100% RH has the lowest. This indicated that the fibres that has been in 0% RH is stronger than the fibres in 100% RH. The standard deviation is highest for 0% while lowest for the 100% which means that the results from the tensile test data is more scattered for 0% RH than for the 100%. To get better result and lower the standard deviation, more fibres must be tested. Since the UTS shows a large gap between the highest value and the lowest value for the different fibres tested in the experiments, the average value for the UTS shows a better understanding of how strong the fibres from the different RH are. It shows, as before, that the fibres in experiment with 0% RH is the strongest, followed by 50%, and 100% gives the weakest fibres.

What Young´s modulus describes is the stiffer the fibre, the higher Young´s modulus value. The young´s modulus value for 0% is the highest, that is to say with less moisture in the fibre, the stiffer the fibres are.

When the fibres contain more moisture they swell and after a certain degree of swelling, the fibers mechanical properties decreased. This might indicate a higher level of sensitivity when exposed to higher moisture levels. Water serving as a softening agent for the wood polymer can explain the drop of Young's modulus as well as UTS with higher RH levels [17].

The source of the changes in mechanical properties can be discovered in the cell wall structure. The cell wall contains of stable and highly stiff cellulose fibrils (around 130 GPa, wet and dry) that are embedded in a softer matrix of hemicelluloses (2 GPa dry, 20 MPa wet) and lignin (2 GPa dry and wet) [5].

Swelling happens transversally to the cellulose fibrils longitudinal axis as they ab-

sorb water. Because the matrix polymers have a lower stiffness and strength than cellulose, the cell wall strength and stiffness in the direction transverse to the fibrils are likewise lower, and this decreases even more when exposed to higher levels of moisture [5]. This might explain why the value for Young´s modulus is almost three times higher for the fibres conditioning in 0% RH compared with the fibres conditioning in 100% RH.

5.2 Weibull statistics

With a higher Weibull modulus, the more consistent is the material, which means that the same "defects" are evenly distributed throughout the entire sample. It also means that it has a narrower probability curve of the strength distribution. The 0% RH test has the highest Weibull modulus value which means that fibres that has been conditioned in lower RH has a more even distribution of defects in the entire sample.

The fibre conditioned under 0% RH has the highest values for UTS and also the highest characteristics strength. The characteristic strength obtained with the help of Weibull statistics is representative regarding the microstructure of the fibres, what defects the fibre has. This means that a conclusion can be drawn that 0% has less defect on the microstructure level than both 50% and 100% has.

5.3 Uncertainties

The fibre that gets extracted can be seen as being stronger than others and therefore, all the fibres might not be as strong as the results show. Since this applies to all the fibres tested, they can still be compared with each other because they have the same conditions.

The RH from the experiment with 0% might not be 0%. The oven was set at 60 degrees to not get any damage on the fibres and also so that the glue would not melt. In the future, putting the fibres in a high vacuum chamber to ensure that it will be 0% humidity is recommended.

The cross-section of fibres is generally non-uniform, which means that it is not the same in all parts or areas of the fibre. This complicates tensile testing, especially when combined with variations in CSA form over the length of the fibre. Furthermore, because failure might occur at any point along the fibre where it is weaker, predicting the breaking point is challenging. It is difficult to get a precise cross-section measurement because of this and this will lead to problems with obtaining correct values of tensile strength and Young's modulus for natural fibres [18]. Furthermore, when using ImageJ to obtain the CSA, the drawn line to create the circle is made by hand and is therefore impossible to be 100% accurate. As a result, CSA might not be accurate.

The aluminum frame does not have the same dimensions in the system compliance test. This is due to a different sizes of the hole in the fame for the different gauge lengths of the fibres. This results in different influence of the aluminum frame on the system compliance for the different tests.

Unfortunately, because the results in this study are real data rather than those created by a random generator, the real values of m and characteristic strength of the fibres can not be 100% accurate. As a result, it is still unclear how near the calculated values of m and characteristic strength are to the genuine ones.

5.4 Development of the method

This thesis is focused on the development of the method to get the best result possible. This chapter is devoted to show the different methods tested that led to the method that was later used.

5.4.1 Selection of supporting frame and glue

Paper frames from regular copy paper and silver glue were used in the beginning. Paper was used since it is stated so in the standard, furthermore also that it is often occurring in the literature. When the paper frame was placed in the tensile machine and the sides were cut, a lot of test fibres broke immediately. This was either due to that the paper was too heavy for the fibre to hold up, or due to that the silver glue was not strong enough so that the fibre was pulled out from it.

The reason that superglue was not used on the paper frame was because the glue wets the paper quick and spreads out too much on the paper. With the aluminum frame it was possible to get a drop of glue on the frame and easily put the fibre in it. The density for paper is 1.20 g/cm^3 and for aluminum foil it is 2.7 g/cm^3. The frame made of aluminum foil is 0.009 mm thick and the frame made from paper is 0.1 mm thick. Thus, the aluminum frame is much lighter than the frame made from paper.

Aluminum foil was chosen as a new frame for many different reasons. The first one was that it is much ridged than paper, so none of the fibres broke during cutting. The second reason was to be able to use super glue to get better adhesion between the glue and the fibre. The last reason was to be able to do in-situ tests. When doing in-situ test, the test samples must be conductive, which aluminum is. The change from silver glue to super glue was also due to the conclusion drawn that silver glue was not strong enough.

5.4.2 Determination of cross-sectional area

Determining the CSA of the fibres was not a simple task. Many attempts were made to develop a reliable high-throughput method and these are described in this section.

5.4.2.1 FIBSEM

An accurate method to determine the CSA was developed early in this project, it was the use of FIBSEM. The fibres were embedded in a resin and with the help of FIB, the fibres were cut very fine to get a smooth surface. The SEM could then image the fibres CSA, an example of this is seen in Figure 5.1, as well as how the CSA is determined with the help of ImageJ. This method is extremely time-consuming, and due to that this project had so many tests carried out and a lot of test bodies that had to be checked for the CSA, a high through-put and high-resolution methods was developed.

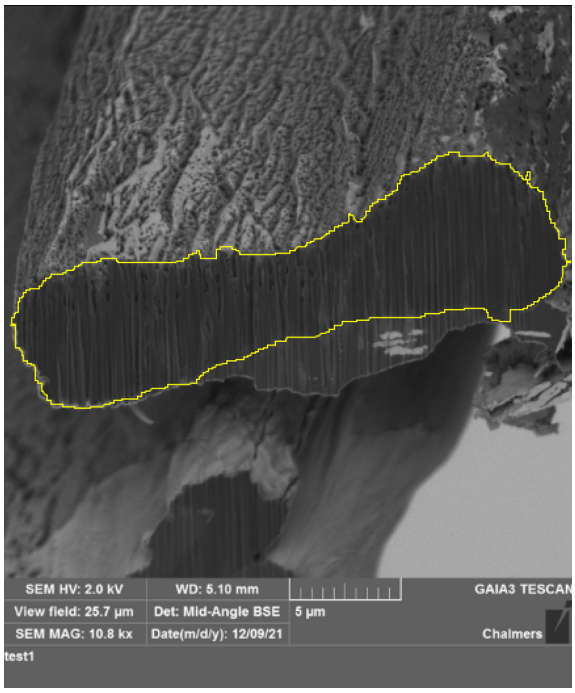

Figure 5.1: FIBSEM and ImageJ used to determine the CSA of a single fibre.

5.4.2.2 Fibre dyeing

Another method to determining the CSA was dyeing the fibres by dipping the fibres in food colouring. After dipped in food coloring, they were dried for a few minutes so that the colour did not spread out to much in the glue before putting the fibres parallel to each other on copper tape. A layer of super glue was placed on top of the fibres and then the glue was dried for at least 24 hours. The fibres are to small to handle directly, therefore must be embedded. After embedding there is no contrast between the fibre and the glue (matrix), therefore food coloring is used to dye the fibre. Figure 5.2 shows a photograph taken with the stero microscope on the fibres on the copper tape in glue.

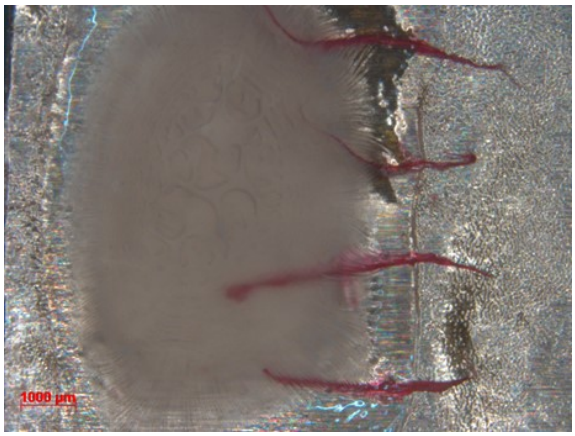

Figure 5.2: Dyed fibres embedded in super glue on a piece of copper tape.

After the glue had dried, the piece of glue, tape and fibres were grind and polished against a sandpaper. First, a rough sandpaper was used and then finer and finer ones to get a flat and fine surface. First a grid size of the sandpaper of 800, followed by 1200 and last 2000 were used. After the preparations were done, the piece was placed under a microscope. Under the microscope the copper tape, the glue and the colored fibres. A image could be distinguished of the fibres was taken, see Figure 5.3. The reason this method was not used was that it was not accurate. The colour could spread in the glue and give a wrong cross-section measurement.

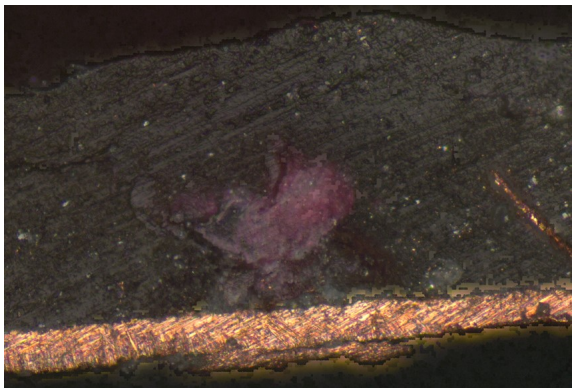

Figure 5.3: Optical photograph of the fibres cross-section.

5.5 Further development

In this section, examples of future development is presented.

5.5.1 In-situ test

In-situ mechanical test procedures that work on samples with micro- or nanometer-scale dimensions have seen great expansion in the utilization of SEM during the last decade. The sample dimensions have a significant impact on the deformation processes, thus it is critical to characterize the mechanical characteristics of a material

at this scale. Therefore, SEM are used in a variety of experiments for observation of sample deformation. [19]

Nanoindentation is a great method for determining the mechanical characteristics of composite fibres in-situ at the micron or sub-micron scale without the need for extraction or material damage. This approach is appealing because it allows measurements to be taken without the need for burning, chemical, or mechanical alterations to separate individual fibres, as is necessary for traditional tensile testing [20].

Digital image correlation (DIC) is an optical technique that does not require any touch of the test specimen to measure strain and displacement. DIC uses digital cameras to capture a succession of images of a surface that has a randomised speckle pattern applied to it. The speckle pattern is transferred to determine the deformed shape in the DIC program, enables derivation of the deflections and stresses of the examined object [21].

5.5.2 Interfacial shear strength

The interfacial shear strength (IFSS) between plant fibers and the polymer matrix is difficult to measure directly. In this context, contemporary technologies such as nanoindentation and atomic force microscopy (AFM) show promise. Single fiber pull-out test, fragmentation test, microbond test, microdroplet test, and push-out test are some of the other methods for determining IFSS. AFM studies can also be used to gather mechanical data at the cell wall scale.

5.5.3 Microfibril angle

As mention in the theory, the MFA is a key component when establishing the physical, for example shrinkage, and mechanical, for example, stiffness and tensile strength, qualities of wood fibres. By using wide-angle X-ray diffraction (WAXD) measurements and tensile testing, the MFA could be determined.

Furthermore, an interesting investigation would be to determine the relationship between cellulose fibril angle and mechanical properties at different moisture contents. Previous research on single wood fibres has revealed that the increase in tensile stiffness with decreased moisture content is more noticeable for cell walls with higher MFAs [5].

5.5.4 Moisture content of the fibres

Check the moisture content of the fibres after they have been conditioned in different RH to see how much water the fibres contain and how that effects the mechanical properties of the fibres.

5.5.5 Fracture surface

Looking at the fracture surface of the fibres after the tensile test to see if there is some difference between the fibres conditioning in the different RH would be an interesting investigation.

6
Conclusion

In this thesis, a robust and high throughput method has been developed to conduct tensile tests to investigate the impact of different humidity conditions on the mechanical properties of single wood fibres.

Using aluminium foil instead of paper allows for a more stable frame as well as more better gluing. Also, super glue tends to have a stronger adhesion to both the aluminium foil as well as the fibre. To determine the CSA of the fibres, the most accurate method was using FIB-SEM as described in 5.4.2.1. Despite its high accuracy, this method is time-consuming. Thus, the method of embedding, scalpel cutting and SEM imaging described in 3.5, is the method that was used instead.

The fibres testing results indicate that with decreased humidity, the UTS as well as Young´s modulus of these wood fibres increases. The Young´s modulus value is higher with less moisture in the fibre. As a result, the stiffer the fibre, the higher young´s modulus value. Water serving as a softening agent for the wood polymer can explain the drop of Young's modulus as well as UTS with higher RH.

The characteristic strength of the fibres suggests that fibres exposed to lower levels of RH has less defect on the microstructure level than fibres exposed to higher levels of RH.

Bibliography

[1] D. Dai and M. Fan. *Natural Fibre Composites*. Elsevier, 2014. Chap. Wood fibres as reinforcements in natural fibre composites: structure, properties, processing and applications. ISBN: 978-0-85709-524-4. DOI: 10.1533/9780857099228.1.3. URL: https://doi.org/10.1533/9780857099228.1.3.

[2] Hiroshi Nishimura et al. "Direct evidence for ether linkage between lignin and carbohydrates in wood cell walls". In: *Scientific Reports* 8 (Apr. 2018). DOI: 10.1038/s41598-018-24328-9. URL: https://www.researchgate.net/publication/324757271_Direct_evidence_for_a_ether_linkage_between_lignin_and_carbohydrates_in_wood_cell_walls.

[3] C.-L Huang et al. "Cell wall structure and wood properties determined by acoustics—a selective review". In: *Holz als Roh- und Werkstoff* 61.5 (Oct. 2003). DOI: 10.1007/s00107-003-0398-1. URL: https://doi.org/10.1007/s00107-003-0398-1.

[4] Andrzej K Bledzki and Omar Faruk. "Creep and impact properties of wood fibre–polypropylene composites: influence of temperature and moisture content". In: 64.5 (Apr. 2004). ISSN: 0266-3538. DOI: 10.1016/S0266-3538(03)00291-4. URL: https://doi.org/10.1016/S0266-3538(03)00291-4.

[5] Nils Horbelt et al. "Effects of moisture and cellulose fibril angle on the tensile properties of native single Norway spruce wood fibres". In: *Wood Science and Technology* 55 (Sept. 2021). DOI: 10.1007/s00226-021-01315-4. URL: https://doi.org/10.1007/s00226-021-01315-4.

[6] Michaela Eder et al. "Experimental micromechanical characterisation of wood cell walls". In: *Wood Sci Technol* 47.1 (Jan. 2013). ISSN: 1432-5225. DOI: 10.1007/s00226-012-0515-6. URL: https://link.springer.com/article/10.1007/s00226-012-0515-6.

[7] Iveta Cabalova et al. *The Effects of Paper Recycling and its Environmental Impact*. American Physical Society (APS), June 2011. ISBN: 978-953-307-358-3. DOI: 10.1051/epjconf/20100620001. URL: https://doi.org/10.1051/epjconf/20100620001.

[8] Xuan Yang. *Eco-friendly Holocellulose Materials for Mechanical Performance and Optical Transmittance*. Royal Institute of Technology, Oct. 2019. ISBN: 978-91-7873-351-4.

[9] ASTM International. *Standards Products*. 2022. URL: https://www.astm.org/products-services/standards-and-publications/standards.html.

[10] ASTM International. "Standard Test Method for Tensile Strength and Young's Modulus of Fibers". In: 15.01 (Jan. 2020). DOI: 10.1520/C1557-20.

[11] Mukesh Kumar Singh and Annika. Singh. *Characterization of Polymers and Fibres*. Elsevier, Sept. 2021. ISBN: 978-0-12-823986-5. DOI: 10.1016/B978-0-12-823986-5.00008-7. URL: https://doi.org/10.1016/B978-0-12-823986-5.00008-7.

[12] Chalmers Univeristy of Technology. *Focused Ion-Beam (FIB)*. 2022. URL: https://www.chalmers.se/en/researchinfrastructure/CMAL/instruments/FIB/FIB/Pages/default.aspx.

[13] Microscope World. *ZEISS SteREO Discovery.V20 Motorized Stereo Microscope*. 2022. URL: https://www.microscopeworld.com/p-3169-zeiss-stereo-discoveryv20-motorized-stereo-microscope.aspx.

[14] Nikolaos Zafeiropoulos and Caroline Baillie. "A study of the effect of surface treatments on the tensile strength of flax fibres: Part II. Application of Weibull statistics". In: *Composites Part A-applied Science and Manufacturing - COMPOS PART A-APPL SCI MANUF* 38 (Feb. 2007). DOI: 10.1016/j.compositesa.2006.02.005. URL: https://www.researchgate.net/publication/248206227_A_study_of_the_effect_of_surface_treatments_on_the_tensile_strength_of_flax_fibres_Part_II_Application_of_Weibull_statistics.

[15] Aparna Roy et al. "Improvement in mechanical properties of jute fibres through mild alkali treatment as demonstrated by utilisation of the Weibull distribution model". In: 107 (Mar. 2012). ISSN: 0960-8524. DOI: 10.1016/j.biortech.2011.11.073. URL: https://doi.org/10.1016/j.biortech.2011.11.073.

[16] SPI Supplies. *Kammrath Weiss Tensile/Compression Module*. 2022. URL: https://www.2spi.com/item/09000-ab/.

[17] B. A.. -L. Östman. "Wood tensile strength at temperatures and moisture contents simulating fire conditionss". In: *Wood Science and Technology* 19 (June 1985). DOI: 10.1007/BF00353071. URL: https://doi.org/10.1007/BF00353071.

[18] Mark C. Symington et al. "Tensile Testing of Cellulose Based Natural Fibers for Structural Composite Applications". In: *SAGE Publications 2009* 43.9 (Jan. 2009). DOI: 10.1177/0021998308097740. URL: https://doi.org/10.1177/0021998308097740.

[19] Nicholas Antoniou, Konrad Rykaczewski, and Michael Uchic. "In situ FIB-SEM characterization and manipulation methods". In: *MRS Bulletin* 39 (Apr. 2014). DOI: 10.1557/mrs.2014.58. URL: https://www.researchgate.

net/publication/269385322_In_situ_FIB-SEM_characterization_and_manipulation_methods.

[20] Alaina Bourmaud et al. “Towards the design of high-performance plant fibre composites”. In: 97 (Aug. 2018). DOI: 10.1016/j.pmatsci.2018.05.005. URL: https://doi.org/10.1016/j.pmatsci.2018.05.005.

[21] Molland Anthony F. and Stephen R. Turnock. *Marine Rudders, Hydrofoils and Control Surfaces Principles, Data, Design and Applications*. Elsevier, 2022. Chap. Chapter 6 - Rudder experimental data. ISBN: 978-0-12-824378-7. DOI: 10.1016/B978-0-12-824378-7.00012-3. URL: https://doi.org/10.1016/B978-0-12-824378-7.00012-3.

A

Appendix 1

Table A.1: Gauge length of the commarcial carbon fibres T800 used to calculate system compliance.

Fibre number:	**Gauge length [μm]:**
1	2544
2	2132
3	2311
4	4413
5	4413
6	4616
7	10402
8	10862
9	10104
10	15610
11	15337
12	15183

Table A.2: Gauge length, CSA, UTS and Young´s modulus for fibres with 0% relative humidity.

Fibre number:	**Gauge length [μm]:**	**CSA [μm^2]:**	**UTS [MPa]:**	**Young´s modulus [GPa]:**
1	1814	317	633	11.99
2	1700	186	1148	11.87
3	1481	413	688	7.35
4	1576	450	1138	14.13
5	1956	312	643	8.26
6	1807	373	813	6.76
7	1677	626	1055	10.13
8	1648	101	1293	16.41
9	2068	426	1110	7.51
10	1459	1195	643	4.01
11	1452	211	651	6.67
12	1494	1044	585	6.89
13	1399	774	605	6.22
14	1845	414	1034	12.17
15	995	696	910	3.88
16	2573	192	1071	12.19
17	1577	464	809	12.16
18	1181	489	789	9.65
19	1592	885	1242	11.70
20	1495	444	878	6.28
21	1734	147	773	7.83
22	1888	413	499	5.69

Table A.3: Gauge length, CSA, UTS and Young´s modulus for fibres with 50% relative humidity.

Fibre number:	**Gauge length [μm]:**	**CSA [μm^2]:**	**UTS [MPa]:**	**Young´s modulus [GPa:**
1	1725	1161	363	2.69
2	1818	1053	365	2.48
3	1742	625	665	4.15
4	1708	377	726	9.05
5	2098	475	385	8.01
6	1546	426	563	4.69
7	1409	943	400	3.03
8	1481	972	576	7.61
9	1919	1098	315	1.98
10	1494	486	312	1.31
11	1966	992	329	3.52
12	1397	340	711	6.20
13	1684	423	782	4.77
14	1527	532	771	6.37
15	1871	466	392	9.41
16	1530	893	626	3.22
17	1937	1238	353	3.82
18	1591	1415	484	2.54
19	2265	309	304	6.16
20	1606	434	570	4.70
21	1883	1028	428	3.24
22	2287	609	701	6.22

Table A.4: Gauge length, CSA, UTS and Young´s modulus for fibres with 100% relative humidity.

Fibre number:	**Gauge length [μm]:**	**CSA [μm^2]:**	**UTS [MPa]:**	**Young´s modulus [GPa]:**
1	1661	885	67	0.62
2	1810	842	236	5.62
3	1218	798	259	2.10
4	2860	637	254	2.37
5	1624	480	95	1.34
6	1970	407	254	5.44
7	1727	602	44	0.26
8	2155	338	93	1.92
9	1491	224	319	2.66
10	1570	1646	389	1.95
11	1605	959	329	4.26
12	1698	1174	127	2.11
13	1934	991	47	0.79
14	1541	664	289	2.54
15	1527	677	319	4.82
16	1580	626	262	3.91
17	1567	481	340	3.92
18	1803	785	319	3.66
19	1573	797	154	1.68
20	1739	2291	334	3.63
21	1503	713	350	3.81
22	2076	537	102	2.94

DEPARTMENT OF INDUSTRIAL AND MATERIALS SCIENCE
CHALMERS UNIVERSITY OF TECHNOLOGY
Gothenburg, Sweden
www.chalmers.se

CHALMERS
UNIVERSITY OF TECHNOLOGY